PURDUE UNIVERSITY
GRADUATE SCHOOL
Thesis/Dissertation Acceptance

This is to certify that the thesis/dissertation prepared

By Shehab Ahmed

Entitled

TRPV4 and cAMP mediated ion transport in the choroid plexus.

For the degree of Master of Science

Is approved by the final examining committee:

Dr. Bonnie Blazer-Yost
Chair

Dr. Teri Belecky-Adams

Dr. Nicolas Berbari

Dr. Charles Gattone

To the best of my knowledge and as understood by the student in the Thesis/Dissertation Agreement, Publication Delay, and Certification Disclaimer (Graduate School Form 32), this thesis/dissertation adheres to the provisions of Purdue University's "Policy of Integrity in Research" and the use of copyright material.

Approved by Major Professor(s): Dr. Bonnie Blazer-Yost

Approved by: Dr. Stephen Randall 12/1/2016

Head of the Departmental Graduate Program Date

TRPV4 AND cAMP MEDIATED ION TRANSPORT IN THE PORCINE CHOROID PLEXUS

A Thesis

Submitted to the Faculty

of

Purdue University

by

Shehab Ahmed

In Partial Fulfilment of the

Requirements for the Degree

of

Master of Science

December 2016

Purdue University

Indianapolis, Indiana

ACKNOWLEDGEMENTS

First of all, I would like to express my sincerest gratitude to Dr. Bonnie Blazer-Yost for accepting me into her laboratory and giving me the opportunity of being part of this truly intriguing research project. I consider myself really lucky to have found her as my mentor. I would like to thank her for her valuable guidance, constant support and encouragement.

I would like to thank the members of my thesis committee, Dr. Teri Belecky-Adams, Dr. Nicolas Berbari and Dr. Charles Goodlett for all their suggestions and advice. They have always been kind and understanding.

I am extremely thankful to my current and previous lab members, Dr. Simon Shim, Stephanie Flaig, Ashley Smith, Ellen Maue, Ayo Otun, Dan Preston, Nalini Kulkarni, Stephanie Simpson and Calen Danko for their help and support. I am also extremely grateful to all my friends and family, especially Shashank Nambiar, A.J. Shih and Asma Salek for their constant support and encouragement.

TABLE OF CONTENTS

LIST OF FIGURES

LIST OF ABBREVIATIONS

AQP1	Aquaporin 1
ATPase	Adenyltriphosphatase
$BaCl_2$	Barium chloride
BK	Big potassium channel
Ca^{2+}	Calcium ion
cAMP	Cyclic adenosine monophosphate
CFTR	Cystic fibrosis transmembrane conductance regulator
Cl^-	Chloride ion
Clir	Inwardly rectifying chloride channel
CNS	Central nervous system
CO_2	Carbondioxide
CP	Choroid Plexus
CPE	Choroid plexus epithelial
CSF	Cerebrospinal Fluid
DIDS	4,4'-Diisothiocyano-2,2'-stilbenedisulfonic acid
DIOA	(Dihydroindenyl)oxy alkanoic acid
DMEM/F12	Dulbecco's modified Eagle's medium/Hams F-12
DMSO	Dimethyl sulfoxide
EDTA	Ethylenediaminetetraacetic acid
ENaC	Epithelial sodium channel
EVD	External Ventricular Drain
FBS	Fetal bovine serum
GlyH-101	glycine hydrazide -101
H2O	Water
HBSS	Hanks Balanced salt solution
HCO_3^-	Bicarbonate
IK	Intermediate conductance calcium-activated potassium channel
K^+	Potassium ion
KCC	Potassium chloride cotransporter
KCNE2	Potassium voltage-gated channel subfamily E member 2 channel
Kir	Inwardly rectifying potassium channel
Kv	Voltage-gated potassium channels
MKS	Meckel-Gruber Syndrome
Na^+	Sodium ion
NBCe2	Electrogenic sodium bicarbonate cotransporter
NBCn2	Sodium-driven chloride bicarbonate exchanger
NCC	Sodium chloride cotransporter

NHE1	Sodium hydrogen exchanger 1
NKCC1	Sodium potassium chloride cotransporter 1
PCP-R	Porcine choroid plexus-resistance
pH	Potential of Hydrogen
SCC	Short circuit current
SGK1	Serum glucocorticoid-induced protein kinase
SK	Small conductance calcium-activated potassium channel
T16Ainh-AO1	Transmembrane member 16A inhibitor- Anoctamin-1
TER	Trans-epithelial resistance
TMEM16A	Transmembrane member 16A
TMEM67	Transmembrane protein 67
TRPV4	Transient receptor potential cation channel subfamily Vanilloid member 4
VRAC	Volume-regulated anion channel
Wpk	Wister polycystic kidney
ZO-1	Zonula occludens-1

ABSTRACT

Shehab, Ahmed. M.S., Purdue University, December 2016. TRPV4 and cAMP Mediated Ion Transport in the Porcine Choroid Plexus. Major Professor: Bonnie Blazer-Yost.

Hydrocephalus is a medical condition characterized by a buildup of cerebrospinal fluid which causes hydrostatic pressure to increase resulting neuronal destruction and can ultimately cause death. Hydrocephalus is seen in both the pediatric population and adults. Treatment of hydrocephalus usually involves surgical placement of a relocation system to drain the fluid into the abdominal cavity. Hydrocephalus may be caused by mechanical obstruction of the outflow of CSF from the ventricles or by faulty reabsorption. It can be also caused by CSF overproduction by the choroid plexus found in the lateral, third, and fourth ventricles of the brain. The choroid plexus is composed of a high resistance monolayer epithelium which surrounds a network of capillaries. Its primary function is to regulate transport of ions and water that control the production and movement of CSF. Therefore it is important to understand the mechanism of CSF production by the choroid plexus. Recently, a stable porcine choroid plexus (PCP-R) epithelial cell line with a high transepithelial resistance (TER) was developed that provides an important model to study regulation of CSF production. Ussing style electrophysiology was used to measure short circuit current (SCC) to characterize stimulated transepithelial ion transport in confluent PCP-R cells. GSK1016790, a TRPV4 agonist, was used to understand the role of TRPV4

in CSF production by the choroid plexus using PCP-R cell model. TRPV4 activation produces a sustained ion transport response that is consistent with an increase in cation secretion and/or anion absorption which is accompanied by a reversible decrease in TER. The effect of the agonist on both SCC and TER was blocked by HC067047, a TRPV4 antagonist, showing that the sustained ion transport and TER change is TRPV4 specific. TRPV4 mediated ion flux was inhibited by CFTR inhibitor II GlyH-101, a cell permeable inhibitor of the cAMP activated chloride channel CFTR, when added on either side of the membrane and was not accompanied by a TER reversal which showed that CFTR is activated by TRPV4 mediated ion flux. TMEM16A, a calcium activated chloride channel, was speculated to be located in that basal membrane as T16Ainh-AO1, a membrane permeable TMEM16A inhibitor, reversed the TRPV4 mediated ion flux when added on either side of the membrane. Slight reversal in TER was observed when T16Ainh-AO1 was added on the apical side. Apamin, a differential inhibitor of calcium activated small conductance potassium channel 1, 2 and 3 (SK1, SK2 and SK3) had no effect on the TRPV4 mediated ion flux. Whereas, fluoxetine, a membrane permeable inhibitor of SK1, SK2 and SK3 channel, inhibited the TRPV4 mediated ion flux and TER change. Bumetanide, an inhibitor of the sodium-potassium-chloride cotransporter reversed TRPV4 mediated ion flux when added on the apical membrane but not on the basal membrane indicating a possible K^+ secretion via SK1 and/or SK4/IK channels and Cl^- absorption through CFTR and TMEM16A channels. Acetazolamide, a carbonic anhydrase inhibitor and a compound used to treat hydrocephalus had no effect on the TRPV4 mediated ion flux. cAMP is an intracellular mediator involved in neuromodulator effects, inflammatory responses and other regulatory mechanisms and is constitutively

activated by forskolin. In PCP-R cells, forskolin stimulated an increase in transepithelial ion flux that is consistent with an increase in cation absorption and/or anion secretion. Forskolin mediated ion transport was inhibited by CFTR inhibitor II GlyH-101 when added on either side of the membrane. No change in TER was observed. No effect on forskolin mediated ion flux was observed when T16Ainh-A01, apamin or fluoxetine were added. Forskolin stimulated transport is partially inhibited by 1 mM $BaCl_2$. Barium chloride is a general inhibitor of K^+ channels. No change in TER was observed.

CHAPTER 1: INTRODUCTION

1.1 Pediatric hydrocephalus

Pediatric hydrocephalus is a medical condition characterized by an accumulation of cerebrospinal fluid (CSF) which triggers an increase in hydrostatic pressure causing neuronal destruction and can ultimately cause death (Schwamb et al., 2014). It affects nearly 1 in 1000 births, and has medical costs approximately $2 billion per year. Hydrocephalus is caused by overproduction, poor absorption, and/or mechanical blockage of the CSF circulation. Based on its mechanisms, hydrocephalus can be classified into two types, communicating and obstructive. Communicating or non-obstructive hydrocephalus is caused by overproduction of CSF by the choroid plexus which overwhelms the reabsorption ability of the arachnoid, as a result there is CSF accumulation in the ventricles of the brain. Obstructive or non-communicating hydrocephalus is caused by an obstruction in CSF flow. The obstruction can be caused by tumors, infections, hemorrhages or congenital malformations in the brain (Huh et al., 2009; Ortloff et al., 2013; Nimjee et al., 2010; Cutler et al., 1973).

Placement of a shunt is the most commonly used treatment for hydrocephalus in which a tube is inserted into the ventricles of the brain which diverts excess CSF into a different region of the body from where it can be absorbed. Abdominal cavity is

generally preferred. To maintain CSF at normal pressure, a valve is used within the shunt system (Yadav et al., 2010). There are a number of complications associated with shunt placement such as infection, obstruction, over drainage, and intraventricular hemorrhage. Many of the complications seen in patients require immediate shunt revision (Drake et al., 2010). Therefore it is of great importance to find an alternative form of treatment to improve patient survival.

1.2 Importance of TRPV4 in hydrocephalus

Transient receptor potential cation channel subfamily vanilloid member 4 (TRPV4) is a non-selective Ca^{2+}-permeable cation channel. Non-selective cation channels are pores in the plasma membrane which form an aqueous passage to allow rapid flow of cation, mainly Na^{+}, K^{+} or Ca^{2+}, determined by the ion selectivity. TRPV4 is permeable to both Ca^{2+} and Na^{+} with 10:1 selectivity under physiological conditions (Plant et al., 2007). TRPV4 is widely expressed in the lung, liver, kidney, spleen, smooth muscle, skin, sweat glands and the central nervous system (CNS) where TRPV4 depolarizes the membrane potential and/or generates a Ca^{2+} signal (Sung et al.,2015; Tyerman, 2002). In the CNS, TRPV4 is expressed in the choroid plexus as well as in the glial and neuronal cells of the cerebral cortex (Shim and Blazer- Yost, unpublished data; Butenko et al., 2012). TRPV4 contributes to crucial systematic and cellular functions such as volume regulation, dilation of arteries, frequency of ciliary beat, etc. via its osmo and mechano transduction properties (Venkatachalam et al., 2007; Song et al., 2010). TRPV4 also responds to various ques such as temperature change, phorbol esters and

arachidonic acid metabolites (endogenous) (Earley et al., 2015). When TRPV4 is activated, the increased intracellular Ca^{2+} activates Ca^{2+}-sensitive channels responsible for transepithelial ion fluxes in the choroid plexus. Unpublished data from our lab shows drugs that act as antagonists to TRPV4, ameliorate hydrocephalus in Wister polycystic kidney (Wpk) rats, when given during the first 18 days after birth (Figure 1.1), which is why it is intriguing to explore the role of TRPV4 in CSF production. Wpk rat is an orthologous model of the human disease called Meckel Gruber Syndrome type 3 (MKS). This rat model is characterized by a mutant form of the protein called transmembrane protein 67 (TMEM67). TMEM67 is a membrane and ciliary protein that is necessary for centriole migration to the luminal surface and development of the primary cilium (Smith et al., 2006). MKS is caused by a mutation in TMEM67 (Garcia-Gonzalo et al., 2011; Sang et al., 2011). In humans and rodents, MKS is an autosomal recessive disease that presents symptoms such as hydrocephalus and renal cystic disease.

1.3 Choroid plexus

The choroid plexus (CP) structure is relatively simple consisting of a solitary layer of low cylindrical to cuboidal epithelial cells. These cells rest on a basement membrane and are linked at the apical surface by junctional complexes, containing tight and adherens junctions, and desmosomes. The CP highly expresses junction proteins such as claudin 2 and claudin 11. Underneath the basement layer lies a system of leaky capillaries which allow water, small molecules and ions to pass into the fluid of each plexus. Thin diaphragms seal these capillaries. An osmotic gradient is created by

transporting ions from blood to CSF or vice versa by the choroid plexus which drives water movement into or out of the ventricles. Transepithelial movement of water in the choroid plexus via transcellular route was shown before, whereby aquaporin 1 in both the apical and basolateral surface aids water movement from the interstitium to the CSF. Water can also move via a paracellular route when the epithelium becomes leaky (Damkier et al., 2013). Hydrocephalus can be caused either by an imbalance of CSF secretion and/or absorption or an obstruction in the CSF flow (Johanson et al., 2008). Therefore understanding the exact role of the ion channels or co-transporters expressed by the CP and the role of TRPV4 is of great importance.

1.4 Ion pumps, channels and cotransporters in the choroid plexus

- Na^+-K^+-ATPase: Na^+-K^+-ATPase is situated in the basolateral surface in most secretory epithelia and mediates the secretion process by creating an inward directed sodium ion gradient which is crucial for the subsequent Cl^- active transport. In contrast, Na^+-K^+-ATPase is located in the apical surface of the CP (Ernst et al., 1986; Masuzawa et al., 1984; Praetorius et al., 2006; Siegel et al., 1984). Apical localization of the Na^+-K^+-ATPase suggests that sodium ion is transported into the CSF and plays an important role in its secretion process. Na^+-K^+-ATPase also functions as a signal transducer to regulate intracellular calcium (Davson et al., 1970; Pollay et al., 1985; Wright et al., 1978). Na^+-K^+-ATPase was shown to be activated by calcium (Yingst, 1988).
- Cl^- channels: Previous studies performed on choroid plexus epithelial cells from rat, mouse, and pig have shown the presence of inward-rectifying anion conductances

(Clir) (Kibble et al., 1996; Kajita et al., 2000 Kibble et al., 1997). Clir channels, whose molecular identity is unknown are shown to be constitutively active and are assumed to play a substantial role in chloride ion efflux at the apical surface. It was also shown that the cystic fibrosis transmembrane conductance regulator (CFTR) is not present in CPE cells (Kibble et al., 1997). Cl^- channels of volume-regulated anion channel (VRAC) category were also identified in CPE cells but the molecular identities of these channels are not known (Kibble et al., 1996; Duran et al., 2010; Kibble et al., 1997).

- K^+ channels: Time-dependent, outward-rectifying conductance (Kv), Kv1.1, Kv1.3 and time-independent, inward-rectifying conductance (Kir), Kir7.1 were identified in the mammalian CP apical surface (Kotera et al., 1994). Recent data indicate that potassium voltage-gated channel subfamily E member 2 (KCNE2) channel also plays a role in the outward-rectifying potassium conductance. All these different potassium channels localize in the luminal surface of rat and mouse CP (Roepke et al., 2011). Presence of small conductance calcium-activated potassium channels (SK) and big potassium channels (BK) are yet to be explored.
- Na^+ channels: Epithelial Na^+ channel (ENaC) is generally expressed in tight epithelia such as renal collecting ducts (Amin et al., 2009; Amin et al., 2005; Leenen et al., 2010; Van Huysse et al., 2012; Wang et al., 2010). Amiloride is a known inhibitor of ENaC (Loffing et al., 2003). Amiloride-sensitive ENaC in CPE was not reported (Damkier et al., 2013).
- Na^+-K^+-Cl^- Cotransporters (NKCCs): Na^+-K^+-Cl^- Cotransporter 1 (NKCC1) facilitates movement of $1Na^+$:$1K^+$:$2Cl^-$ across the cell membrane and is bumetanide sensitive (Russell, 2000). NKCC1 is located in the basolateral surface in most secretory

epithelia and facilitates ion influx. However, NKCC1 is expressed in the apical surface of choroid plexus epithelial cells (Plotkin et al., 1997; Keep et al., 1994). It was previously proposed that the force that drives NKCC1 in choroid plexus is near equilibrium (Keep at al., 1994). But other studies have shown that NKCC1 is involved in both ion efflux and influx (Crum et al., 2012; Bairamian et al., 1991). Thus the role of NKCC1 in choroid plexus and CSF secretion is not well understood.

- K^+-Cl^- Cotransporters: KCCs are shown to be electroneutral and enable ion efflux which is driven by a potassium ion concentration difference across plasma membrane. CPE cells were shown to express both KCC3a and KCC4 in the basolateral and the luminal surface respectively (Chai et al., 1987; Millar et al., 2007). Therefore KCC4 might be contributing to the recycling of potassium ions across the apical surface and thus keeping the sodium-potassium-ATPase active. KCC3 is reported to be the only potassium channel expressed in the CPE basolateral surface thus mediating K^+ efflux (Millar et al., 2007).
- Na^+-HCO_3^- Cotransporters: Depending on tissue-specific factors, electrogenic sodium bicarbonate cotransporter (NBCe2) facilitates the movement of two or three HCO_3^- with one Na^+ and is expressed in the luminal surface (Virkki et al., 2002; Sassani et al., 2002;). Sodium-driven chloride bicarbonate exchanger (NBCn2) protein is localized in the basolateral surface of the CP and contributes to cellular accumulation of Na^+ and HCO_3^- (Praetorius et al., 2006; Praetorius et al., 2004). NBCn1 is electroneutral and is reported in the basolateral surface of CP epithelial cells (Praetorius et al., 2004).
- Na^+/H^+ Exchangers: Na^+/H^+ exchanger 1 (NHE1) is shown to be an electrically neutral acid extruder. Immunohistochemical studies have showed that NHE1 is located in

the luminal surface of both human and mouse CP (Kao et al., 2011; Damkier et al., 2009).

- Intracellular mediators: Very little is known about intracellular mediators in the choroid plexus. The only known intracellular mediator in CP is the carbonic anhydrase which catalyses the reversible conversion of water and carbon dioxide to hydrogen ion and bicarbonate. This reversible reaction maintains acid-base balance in blood and other tissues, which helps to transport carbon dioxide out of tissues. Acetazolamide is known to inhibit carbonic anhydrases and reduce CSF secretion by 50 to100% in rats and rabbits. It is also utilised in children and adults to treat hydrocephalus (Davson et al., 1970; Ames et al., 1965; Welch et al., 1963). The drug is thought to act by varying blood flow to the CP (Vogh et al., 1987; Jafarzadeh et al., 2014; Cowan et al., 1991).

Ion distribution between CSF and plasma show that they are not similar. K^+, HCO_3^-, and Ca^{2+} concentrations are lesser in the CSF, while concentration of Cl^- (~ 130mM) is higher in the CSF (Davson et al., 1996). Transportation of these ions create a slight osmotic gradient, which drives the secretion of water. Therefore it is understandable that the movement of ions in the CP is tightly regulated. It was shown before that in mammals, the transepithelial potential difference is +5 mV apical positive (Held et al., 1964; Husted et al., 1977; Welch et al., 1965).

1.5 Objective

The overall objective of the proposed research is to understand ion transport in the choroid plexus, particularly the effect on CFTR, TMEM16A, SK and BK channels in

response to TRPV4 mediated calcium influx and forskolin induced cAMP. It was hypothesised that the above ion channels and cotransporters are activated by TRPV4 mediated calcium influx and forskolin induced cAMP. Role of NKCC1 was also examined. In addition, these studies will provide evidence for using TRPV4 antagonist as a possible treatment option for hydrocephalus and the underlying mechanism of action of the drug.

CHAPTER 2: MATERIALS AND METHODS

2.1 Materials

Transwell culture plates containing 24mm inserts made from polycarbonate (0.4µm pore size) and cell culture flasks were acquired from Costar-Corning (Acton, MA). DMEM/ F12 (Dulbecco's modified Eagle's medium/Hams F-12) tissue culture media, streptomycin, insulin and penicillin were purchased from ThermoFisher Scientific (Waltham, MA). Trypsin-EDTA solution was obtained from Sigma Aldrich (St. Louis, MO). HBSS (Hanks Balanced salt solution) was obtained from Mediatech (Herndon, VA). FBS (Fetal bovine serum) was acquired from Atlanta Biologicals (Atlanta, GA). CFTR Inhibitor II GlyH-101 was acquired from Calbiochem-Merck (Darmstadt, Germany). Forskolin was purchased from Biomol International (Plymouth Meeting, PA). T16Ainh-AO1 and HC 067047 were obtained from Tocris Bioscience (Bristol, UK). $BaCl_2$, GSK1016797, bumetanide, fluoxetine, apamin, and acetazolamide were purchased from Sigma Aldrich (St. Louis, MO).

2.2 Cell culture

The PCP-R (porcine choroid plexus) cell line, passage 47, was obtained from Prof. Christian Schwerk at Heidelberg University, Germany. This cell line is suitable for choroid plexus electrophysiological studies as it is characterized by a high transepithelial resistance (~1500 Ω.cm2) (Schroten et al., 2012). 150 cm^2 tissue culture flasks were used to culture cells in a humidified incubator maintained at 37ºC that consists of 5% CO_2. The culture medium was composed of glucose (4.5 g/L), DMEM, FBS (10%), penicillin (100 U/ml), streptomycin (100 mg/ml) and insulin at 5mg/L. The medium was replaced three times per week. A 0.5% trypsin-EDTA solution was used to passage cells every week at a 1:10 split ratio. Approximately 1.29 million cells were seeded on transwell inserts with 1.5 ml of media on the apical side and 2 ml on the basolateral side and were used on day 10 to 12 to perform electrophysiology. The mean TER of confluent monolayer of cells varied between 500 and 3000 Ω/cm^2.

2.3 Electrophysiology

In order to observer changes in ion movement across the PCP-R epithelia when different inhibitors and stimulators are added, electrophysiology experiments were performed. For electrophysiology experiments, confluent monolayers of PCP-R cells were cultured on transwell membranes for 10 to 12 days. After which the membranes were removed and fitted in an Ussing chamber. Ussing chamber is an apparatus that separates the basolateral surface from the luminal surface. A confluent layer of epithelial

cells become polarized when it's apical and basolateral membrane proteins are segregated on the appropriate membrane. Basal surface is the surface that faces the basement membrane. In transwell, the surface of the cell that is against the filter is the basal surface. Voltage and current electrodes were attached on either side of filters contained in Ussing chamber which were linked to the DVC-1000 voltage/current clamp via electrodes. DVC-1000 was obtained from World Precision Instruments (Sarasota, FL). PCP-R cells were kept at 37ºC and were covered in medium which is free of serum. Constant pH maintenance and circulation of media was performed using a 5% carbon dioxide and 95% oxygen gas cylinder. The short circuit current (SCC) was constantly monitored after the transepithelial potential difference was held at zero. SCC is a quantification of net transepithelial ion movement where an increase denotes either anion secretion and/or cation absorption whereas a decrease denotes either cation secretion and/or anion absorption. 2mV pulses were induced every 200 seconds for 2 seconds and the current displacement during the pulse was used to calculate transepithelial resistance (TER) via Ohm's law. After the cells show a stable basal SCC, compounds such as TRPV4 agonist (GSK1016797), TRPV4 antagonist (HC067047), CFTR Inhibitor II GlyH-101, TMEM16A inhibitor (T16Ainh-A01), Na^+-K^+-Cl^- cotransporter 1 (NKCC1) inhibitor bumetanide, small conductance calcium-activated potassium channel inhibitors such as fluoxetine and apamin, and acetazolamide, which is a carbonic anhydrase inhibitor previously reported to be used to treat hydrocephalus (Carrion et al., 2001), cAMP inducer (forskolin), and nonspecific potassium channel inhibitor ($BaCl_2$) were added to specific sides of the polarized epithelia as indicated in the figures.

2.4 Statistics

Statistical comparison between experimental and control treatments (change in SCC and TER) were done using Student's t-test. Results were considered significant at $p \leq 0.05$.

CHAPTER 3: RESULTS

3.1: Effect of TRPV4 agonists on confluent cultures of PCP-R

In order to determine the membrane localization of the TRPV4 channel, 5nM of TRPV4 agonist (GSK1016797) was added either on the apical or basal side of the polarized epithelia. Upon activation by the agonist, TRPV4 stimulated an increase in cation secretion and/or anion absorption when added on the basal side but not on the apical side. This implies that TRPV4 might be located in the basolateral membrane (Figure 3.1). However, in Figure 3.2 A, HC067047 (TRPV4 specific antagonist) was more potent when added on the apical side compared to the basal side suggesting that TRPV4 might be located on the apical membrane, which is consistent with previous finding that TRPV4 is predominantly localized in the apical surface of the CP (Takayama et al., 2014). This discrepancy in TRPV4 localization in the PCP-R might be due to the intracellular mode of action of the agonist. It is possible that the basally added agonist crossed the basolateral membrane of the polarized PCP-R and activated the apically located TRPV4 as it was shown before that the basal membrane is more permeable compared to the apical membrane (Flamion et al., 1990; Giepman et al., 2009). Immunolocalization experiments targeting TRPV4 are necessary to validate this finding.

GSK1016797 was added on the basal side of the membrane in subsequent experiments as it produced a TRPV4 response only from that side.

3.2: GSK1016790A mediated ion flux and TER decline is TRPV4 specific

To examine if the change in SCC and TER are TRPV4 agonist specific, 5nM of GSK1016797 and 100nM of HC067047 were added either on the apical or basal side of the polarized epithelia. Upon activation by the agonist, TRPV4 stimulated an increase in cation secretion and/or anion absorption. This response was accompanied by a reversible decrease in TER. The effect of the agonist on both SCC and TER was blocked by pre-treatment of the TRPV4 antagonist HC067047 (100nM). HC067047 also fully reversed the agonist stimulated ion flux and considerably restored the agonist stimulated decrease in TER when added after the agonist stimulation (Figure 3.2). This indicates that the change in SCC and TER are TRPV4 agonist specific.

3.3: TRPV4 agonist dose response

To determine the optimum TRPV4 agonist (GSK1016797) concentration, a limited set of dose response experiments were performed. TRPV4 agonist of 1nM, 1.8nM, 3.3nM, 5.6nM or 10nM was added to the basolateral or apical side of the polarized epithelia. When GSK1016790A was added to the basolateral bathing media at a final concentration of 1nM and 1.8nM, there was no indication of ion flux and TER change. Addition of 10nM produced a lethal ion flux as depicted by a drastic decrease in

TER. The addition of 3.3nM and 5.6nM of agonist was not found to be lethal as the TER did not drop below 500 ohm.cm^2. 5nM was the concentration used in subsequent experiments.

3.4: Effect of GSK1016790A on CFTR and TMEM16A

To examine if any chloride channel such as CFTR and TMEM16A are activated by the TRPV4 mediated calcium influx, CFTR Inhibitor II GlyH-101 (50nM) and the TMEM16a inhibitor, T16Ainh-A01 (10µM) were added on either side of the membrane. As mentioned before, TRPV4 agonist mediated change in SCC represents an increase in cation such as K^+ secretion into the CSF side (apical) and/or anion such as Cl^- absorption into the blood side (basal). In this ion flux, the final barrier that a cation has to cross to get secreted into the CSF is a cation channel or co-transporter located on the apical membrane. Similarly, the final barrier that an anion has to cross to get absorbed into the blood is an anion channel or co-transporter located on the basal membrane. Based on this principle, it can be concluded that the anion channels, CFTR and TMEM16A might be located on the basal side as a reversal in the TRPV4 mediated ion flux was observed when DMSO prepared, membrane permeable CFTR or TMEM16A inhibitors were added on either side of the membrane. The inhibitors had an effect when added on the apical side as DMSO preparation made them membrane permeable and allowed them to act on the basal surface. Addition of the CFTR inhibitor on the apical side had an immediate effect whereas a delayed inhibition was observed when added on the basal side. No reversal in TER was observed (Figure 3.5). Interestingly, pre-treatment with CFTR

inhibitor caused a decrease in the TER (Figure 3.5 C). TRPV4 agonist mediated ion flux was reversed immediately by the TMEM16A inhibitor when added on either side of the membrane (Figure 3.6). T16Ainh-A01 partially reversed the decrease in TER caused by TRPV4 agonist when added on the apical side of the membrane (Figure 3.6 D). This was surprising as such reversal was not observed when T16Ainh-A01 was added on the basal side. Localization of CFTR and TMEM16A needs to be verified by immunostaining.

3.5: Role and localization of NKCC1 in PCP-R

NKCC1 is located in the apical membrane of the CP and mediates ion influx of one sodium ion, one potassium ion, and two chloride ion across the plasma membrane (Johanson et al., 1990; Wu et al., 1998; Keep et al., 1994). It was shown before that NKCC1 is constitutively active under physiological conditions (Crum et al., 2012; Wu et al., 1998). To identify the localization and to understand the ion movement mediated by NKCC1 in polarized PCP-R, 100μM of bumetanide was added on either side of the polarized epithelia after TRPV4 activation. TRPV4 mediated ion flux represents an increase in cation such as K^+ secretion into the CSF side (apical) and/or anion such as Cl^- absorption into the blood side (basal) which was reversed by bumetanide when added on the apical side but not on the basal side (Figure 3.7B). This implies that NKCC1 might be located in the apical membrane and Cl^- entering the cell via NKCC1 might leak out through CFTR and TMEM16A channels located on the basal membrane as identified in section 3.4. K^+ ion entering the cell via NKCC1 might leak out through potassium channels on the apical membrane which will be identified in section 3.7. It was shown

before that Na^+ ion entering the cells via NKCC1 is pumped out by the apical Na^+/K^+-ATPase (Johanson et al., 1990; Wu et al., 1998; Keep et al., 1994). Immunostaining is required to verify the NKCC1 localization. It was expected to observe a decrease from the basal current when the polarized epithelia was pre-treated with bumetanide on the apical side as NKCC1 was reported to be constitutively active, surprisingly no such deviation was observed (Figure 3.7A). Figure 3.7A also show that bumetanide pre-treatment did not affect TRPV4 mediated ion flux. Addition of bumetanide did not cause any change in TER (Figure 3.7 C, D).

3.6: TRPV4 mediated ion flux and TER decline is not effected by Acetazolamide

Acetazolamide is known to inhibit carbonic anhydrases and reduce CSF secretion in rats and rabbits. It is currently being utilised in children and adults to treat hydrocephalus (Davson et al., 1970; Ames et al., 1965; Welch et al., 1963). Therefore it was intriguing to find out if TRPV4 mediated ion flux was affected by acetazolamide. Figure 3.8 shows a partial but statistically non-significant reversal of SCC and TER when acetazolamide was added on the apical side but not on the basal side of the polarized epithelia.

3.7: Effect of GSK1016790A on SK channels

There are four known types of SK channels, SK1, SK2, SK3, and SK4. SK4 is also known as IK or Intermediate conductance calcium-activated potassium channel.

Fluoxetine is membrane permeable and a specific blocker of SK1, SK2 and SK3 channels (Kohler et al., 1996; Faber et al., 2007; Stackman et al., 2002). Apamin is also membrane permeable and a differential blocker of SK1, SK2 and SK3 channels. SK2 is the most sensitive, SK3 shows intermediate sensitivity and SK1 is the least apamin sensitive with effective concentration values of ~40pM, ~1nM and ~10nM respectively (Adelman et al., 2012). It was also reported that the cloned SK1 channel is not blocked by 100nM of apamin (Bond et al., 1999). To determine if any small conductance calcium-activated potassium (SK) channels were activated by the TRPV4 mediated calcium influx, either fluoxetine or apamin were added on either side of the membrane before or after TRPV4 stimulation. TRPV4 agonist mediated change in SCC represents an increase in cation secretion into the CSF side (apical) and/or anion absorption into the blood side (basal) which was immediately blocked by fluoxetine on either side of the membrane as it is membrane permeable. This suggests that fluoxetine sensitive SK channels might be located on the apical side which needs to be verified by immunostaining. Pre-treatment of cells with fluoxetine also inhibited TRPV4 agonist mediated ion flux. Reversal in TER was also observed when fluoxetine was added on either side of the membrane. Interestingly, addition of apamin had no effect on the TRPV4 mediated SCC or TER change (Figure 3.9). This finding indicates that TRPV4 mediated calcium influx might activate SK1 and/or SK4/IK channel. Future electrophysiological experiments using specific SK4 channel inhibitor such as Paxilline are required.

3.8: Effect of forskolin on CFTR and TMEM16A

Forskolin is a compound known to activate adenylyl cyclase and increase intracellular cAMP. To examine if chloride channels such as CFTR and TMEM16A are activated by cAMP, CFTR Inhibitor II GlyH-101 (50nM) or T16Ainh-A01 (10μM) were added on either side of polarized PCP-R. Forskolin mediated change in SCC represents an increase in transepithelial ion flux that is consistent with an increase in anion secretion into the CSF side (apical) and/or cation absorption into the blood side (basal). In forskolin mediated ion flux, the last barrier that an anion has to cross to get absorbed into the CSF is an anion channel or co-transporter located on the apical membrane. Likewise, the final barrier that a cation has to cross to get absorbed into the blood is a cation channel or co-transporter located on the basal membrane. Using this notion, it can be concluded that the anion channel, CFTR might be located on the apical side as an immediate reversal in the forskolin mediated ion flux was observed when DMSO prepared, membrane permeable CFTR inhibitor was added on either side of the membrane. DMSO preparation made the inhibitor membrane permeable and allowed it to act on the apically located CFTR which is why the inhibitor was able to reverse the current when added on the basal side (Figure 3.11). Treatment with TMEM16A inhibitor had no effect on forskolin mediated ion flux (Figure 3.12). Neither the stimulatory nor the inhibitory responses were accompanied by a change in TER.

3.9: Role and localization of NKCC1 in PCP-R

It was reported before that under physiological conditions NKCC1 is constitutively active (Wu et al., 1998; Crum et al., 2012). Polarized PCP-R epithelia was pre-treated with bumetanide on either side of the membrane. As expected, a slight but statistically non-significant decrease from the basal current was observed when bumetanide was added on the apical side but not on the basal side (Figure 3.13A). This supports out finding from section 3.5 that NKCC1 might be located on the apical membrane. It might also be implied from this data that NKCC1 might be constitutively active in PCP-R and it might play a role in maintaining a stable basal current. No inhibition in forskolin mediated ion flux was observed. No change in SCC was observed when bumetanide was added on either side of the membrane after forskolin treatment (Figure 3.13B). No change in TER was also observed (Figure 3.13 C, D).

3.10: Effect of forskolin on barium sensitive potassium channels

To identify cAMP dependent potassium channels, forskolin (5µM) and barium chloride (1mM) were added on either side of the membrane. There was an immediate increase in SCC after forskolin addition which was blocked by barium chloride when added on the basolateral side but not on the apical side (Figure 3.14 A, B). This piece of data supports the presence of cAMP dependent potassium channels in the basolateral membrane. These changes in SCC were not accompanied by a change in TER. (Figure 3.14 C, D)

CHAPTER 4: DISCUSSION

Pediatric hydrocephalus is a medical condition characterized by an accumulation of CSF that triggers a rise in hydrostatic pressure causing neuronal destruction and can ultimately cause death. Preliminary data from our lab shows that drugs that act as antagonists to the TRPV4 Ca^{2+} channel ameliorate hydrocephalus in Wpk rats. Wpk rat is an orthologous model of the human disease called Meckel Gruber Syndrome type 3 (MKS). This rat model is characterized by a mutant form of the protein called TMEM67. TMEM67 is a membrane and ciliary protein that is necessary for centriole migration to the luminal surface and development of the primary cilium (Smith et al., 2006). MKS is caused by a mutation in TMEM67 (Garcia-Gonzalo et al., 2011; Sang et al., 2011). In humans and rodents, MKS is an autosomal recessive disease that presents symptoms such as hydrocephalus and renal cystic disease. In the central nervous system, Expression of TRPV4 was observed in the CP, as well as in the glial and neuronal cells of the cerebral cortex (Shibasaki et al., 2007). When activated, TRPV4 transports Ca^{2+} into cells, activating intracellular Ca^{2+} signaling processes and depolarizing the membrane potential. The increased intracellular Ca^{2+} then activates Ca^{2+}-sensitive channels those are responsible for transepithelial ion fluxes in the choroid plexus. Our current study has enabled us to understand ion transport in the choroid plexus, particularly in response to

TRPV4 activation and cAMP and has also aided us to examine the potential use of a TRPV4 antagonist as a treatment option of hydrocephalus.

Recent studies have measured TER of 150 to 200 $\Omega \cdot cm^2$ in mammalian CP cell culture using epithelial volt-ohmmeter (Zheng et al., 2002). However, resistances of up to 2,000 $\Omega \cdot cm^2$ were observed in tight epithelia in which there is a controlled paracellular transport (Whittembury et al., 1985; Rosenthal et al., 2010; Will et al., 2008). In that regard, the PCP-R cell line is suitable to study regulated ion transport in choroid plexus as in our experiments it showed high resistance values between 500 and 3000 $\Omega \cdot cm^2$. The TER of an epithelia is important as it shows how controlled paracellular transport is in that epithelia. It also determines the paracellular permeability. One possible reason for higher TER in the PCP-R cell line is due to higher expression of tight junction proteins such as ZO1, Occludin, Claudin 1 and Claudin 3, etc. which produces a continuous tight junction strand (Schroten et al., 2012).

Previous studies have identified TRPV4 channel in the choroid plexus and was found to be predominantly expressed in the luminal surface (Takayama et al., 2014). In our current electrophysiological experiments, we have found that TRPV4 might be located in the basal membrane of the PCP-R as the TRPV4 agonist was only effective when added on the basal side but not on the apical side. On the other hand, the TRPV4 antagonist was found to be more effective when added on the apical side compared to the basal side suggesting that TRPV4 might be located on the apical membrane, which is consistent with the previous report. This inconsistency in our TRPV4 localization data might be due to the intracellular mode of action of the agonist. It was shown before that the basal membrane is more permeable compared to the apical membrane, therefore it is

possible that the basally added agonist crossed the basolateral membrane of the polarized PCP-R and activated the apically located TRPV4 (Flamion et al., 1990; Giepman et al., 2009). Immunostaining needs to be done to verify this finding. Upon activation by the agonist, TRPV4 stimulated an increase in cation secretion and/or anion absorption when added to the basal side but not the apical side. This change in SCC was also accompanied by a reversible decrease in the TER. Pre and post treatment with a TRPV4 antagonist suggests that the change in SCC and TER are TRPV4 agonist specific.

Previous studies performed on choroid plexus epithelial cells have shown the presence of Clir (Kibble et al., 1996; Kajita et al., 2000 Kibble et al., 1997). Cl^- channels of VRAC category were also identified in CPE cells but the molecular identities of these channels are not known (Kibble et al., 1996; Duran et al., 2010; Kibble et al., 1997). In our current study, we have identified two Ca^{2+} (TMEM16A and CFTR) and one cAMP (CFTR) sensitive chloride channels. The Ca^{2+} sensitive TMEM16A and CFTR channels are thought be located on the basal surface whereas the cAMP sensitive CFTR channel might be located on the apical membrane. Immunostaining is required to verify this finding. CFTR is not known to be directly activated by calcium, however it is possible that it was activated by calcium dependent adenylyl cyclase catalyzed cAMP. Isoforms 3, 5 and 8 of adenylyl cyclase are activated by calcium (Halls et al., 1988). It was reported before that the CFTR mRNA was not detected in rat CP which contradicts with our current finding that CFTR channel is present in the PCP-R. This could be due to non-specific inhibition by the CFTR Inhibitor II GlyH-101 which needs to be verified by performing electrophysiology experiments using CFTR knockout PCP-R cells and also by performing immunostaining targeting CFTR.

Our current study pointed towards the involvement of a barium sensitive, cAMP activated potassium channels in the basolateral side of the PCP-R. It's worth noting that none of these experiments using K^+ channel blockers was accompanied by a change in TER. Data from our experiments also suggests the localization of SK1 and/or SK4/IK channel in the apical membrane of PCP-R. There was no reversal of TRPV4 agonist mediated ion flux by apamin, a differential blocker of SK1, SK2 and SK3 channels (Adelman et al., 2012). Cloned SK1 channel is insensitive to 100nM of apamin (Bond et al., 1999). Addition of fluoxetine, an inhibitor of SK1, SK2 and SK3 channels completely reversed the change in SCC mediated by TRPV4 activation when added on either side of the membrane (Faber et al., 2007; Kohler et al., 1996; Stackman et al., 2002). This suggests a possible localization of SK1 and/or SK4/IK channel in the apical side of the membrane. TRPV4 mediated TER decrease was slightly reversed by fluoxetine. In order to identify SK4 or IK channel, experiments using specific inhibitors need to be performed along with immunostaining. Iberiotoxin, a big potassium (BK) channel inhibitor did not reverse the ion flux caused by TRPV4 agonist or forskolin suggesting an absence of calcium or cAMP dependent BK channel (data not shown). Absence of BK channel needs to be verified using Paxilline, another BK channel inhibitor (Zhou et al., 2014).

Our current study identified a possible localization of NKCC1 on the apical membrane of the PCP-R which is consistent with previous reports (Wu et al., 1998; Gagnon et al., 2012; Damkier et al., 2012). We also observed that Cl^- entering the cell via NKCC1 might leak out through CFTR and TMEM16A channels located on the basal membrane whereas K^+ might leak out through SK1 and/or SK4/IK channels located on the apical membrane. It was proposed before by Wu et al. that Cl^- entering the cell

through NKCC1 is secreted into the CSF via an apical chloride channel and K^+ entering the cell through NKCC1 is reabsorbed in to the blood side via a postulated, basally located potassium channel or co-transporter in isolated, polarized rat CP epithelial cells. These findings are not supported by our current study as we observed secretion of K^+ and reabsorption of Cl^-. A more recent study conducted by Gagnon et al. showed Cl^- reabsorption on the basolateral side via KCC in choroid plexus epithelial cells which is partially consistent with our study as we also identified Cl^- reabsorption but via CFTR and TMEM16A channels. The group also reported K^+ reabsorption via KCC and potassium channel on the basal membrane which is inconsistent with our current study. Other cotransporters and exchangers such as KCC, NBCe2, NCC3 and NHE1 need to be identified by using specific inhibitors such as DIOA, DIDS, Furosemide respectively (Damkier et al., 2013). Previous studies showed that NKCC1 is constitutively active under physiological conditions (Wu et al., 1998; Crum et al., 2012). Our current study might agree with this notion as we noticed a statistically non-significant decrease from the basal current when PCP-R epithelia was treated with bumetanide on the apical side before forskolin treatment.

Acetazolamide inhibits carbonic anhydrases activity and reduces CSF secretion in rats and rabbits. Children and adults are administered with acetazolamide to treat hydrocephalus. So it was intriguing to find out if TRPV4 mediated ion influx can be inhibited by acetazolamide which will indicate a possible activation of carbonic anhydrase by TRPV4 activity in PCP-R. Our data suggests no modulation of carbonic anhydrase by TRPV4 activation. Forskolin mediated current was not found to be effected by acetazolamide (data not shown).

CHAPTER 5: FUTURE DIRECTIONS

Our current data warrants a fair amount of future experiments in order to hone on the mechanism and function of TRPV4 in CSF production. Recent electrophysiological experiments on renal cells in our lab suggest the involvement of serum glucocorticoid-induced protein kinase-1 (SGK1) in TRPV4 regulation. SGK1 has been shown before to be important in activating certain sodium, potassium and chloride channels (Webster et al., 1993). It was also shown that TRPV4 comprises a phosphorylation site on the Ser 824 and is an SGK1 substrate. Ser 824 has been shown to control membrane localization and protein interaction between TRPV4 and calmodulin. This suggests that phosphorylation on TRPV4's Ser 824 can regulate its functions (Lee et al., 2010). TRPV4 regulation by SGK1 in the choroid plexus is yet to be explored.

Our current PCP-R culture and electrophysiology experiments were done using standard cell culture media which is different in terms of ion concentration and pH compared to plasma and CSF (Ding et al., 2016; Davson et al., 1996). Therefore it would be interesting to repeat the experiments using artificial CSF on the apical side and artificial plasma on the basolateral side. These experiments will provide more physiologically relevant data. Repeating the electrophysiology experiments using a human CPE cell line (Schwerk et al., 2012) would be interesting and our laboratory has recently obtained such a line.

REFERENCES

REFERENCES

Adelman JP, Maylie J, Sah P. Small-conductance Ca^{2+}-activated K^{+} channels: form and function. Annu. Rev. Physiol. 74: 245–69, 2012.

Ames A 3rd, Higashi K, Nesbett FB. Effects of pCO2 acetazolamide and ouabain on volume and composition of choroid-plexus fluid. J Physiol 181: 516–524, 1965.

Amin MS, Reza E, Wang H, Leenen FH. Sodium transport in the choroid plexus and salt-sensitive hypertension. Hypertension 54: 860–867, 2009.

Amin MS, Wang H, Reza E, Whitman SC, Tuana BS, Leenen FHH. Distribution of epithelial sodium channels and mineralocorticoid receptors in cardiovascular regulatory centers in rat brain. Am J Physiol Regul Integr Comp Physiol 289: R1787–R1797, 2005.

Bairamian D, Johanson CE, Parmelee JT, Epstein MH. Potassium cotransport with sodium and chloride in the choroid plexus. J Neurochem 56: 1623–1629, 1991.

Bond CT, Maylie J, Adelman JP. Small-conductance calcium-activated potassium channels. Ann. N. Y. Acad. Sci. 868 (1): 370–8, 1999.

Butenko O, Dzamba D, Benesova J, Honsa P, Benfenati V, Rusnakova V, Ferroni S, Anderova M. The Increased Activity of TRPV4 Channel in the Astrocytes of the Adult Rat Hippocampus after Cerebral Hypoxia/Ischemia. PLoS One. 2012; 7(6): e39959, 2012.

Carrion E, Hertzog J, Medlock M, Hauser G, Dalton H. Use of acetazolamide to decrease cerebrospinal fluid production in chronically ventilated patients with ventriculopleural shunts. Arch Dis Child. 84(1): 68–71, 2001.

Chai SY, McKinley MJ, Mendelsohn FA. Distribution of angiotensin converting enzyme in sheep hypothalamus and medulla oblongata visualized by in vitro autoradiography. Clin Exp Hypertens A 9: 449–460, 1987.

Cowan F, Whitelaw A. Acute effects of acetazolamide on cerebral blood flow velocity and pCO2 in the newborn infant. Acta Paediatr Scand. 80(1):22-7, 1991.

Crum JM, Alvarez FJ, Alvarez-Leefmans FJ. The apical NKCC1 cotransporter debate (Abstract). FASEB J 26: 881–814, 2012.

Cutler RW, Murray JE, Moody RA. Overproduction of cerebrospinal fluid in communicating hydrocephalus. A case report. Neurology 23(1):1-5, 1973.

Damkier HH, Brown PD, Praetorius J. Cerebrospinal fluid secretion by the choroid plexus. Physiol Rev. 93(4):1847-92, 2013.

Damkier HH, Prasad V, Hubner CA, Praetorius J. Nhe1 is a luminal Na^+/H^+ exchanger in mouse choroid plexus and is targeted to the basolateral membrane in Ncbe/Nbcn2-null mice. Am J Physiol Cell Physiol 296: C1291–C1300, 2009.

Davson H, Segal MB. Physiology of the CSF and Blood-Brain Barriers. Boca Raton, FL: CRC, 1996, p. 1832.

Davson H, Segal MB. Physiology of the CSF and Blood-Brain Barriers. Boca Raton, FL: CRC, 1996, p. 1832.

Davson H, Segal MB. The effects of some inhibitors and accelerators of sodium transport on the turnover of ^{22}Na in the cerebrospinal fluid and the brain. J Physiol 209: 131–153, 1970.

Ding F, O'Donnell J, Xu Q, Kang N, Goldman N, Nedergaard M. Changes in the composition of brain interstitial ions control the sleep-wake cycle. Science 29;352(6285):550-5, 2016.

Drake, J. M.; Kestle, J. R. W.; Tuli, S. CSF shunts 50 years on - past, present and future. Child's Nervous System 16 (10-11): 800–4, 2010.

Duran C, Thompson CH, Xiao Q, Hartzell HC. Chloride channels: often enigmatic, rarely predictable. Annu Rev Physiol 72: 95–121, 2010.

Earley S, Brayden JE. Transient Receptor Potential Channels in the Vasculature. Physiol Rev 95: 645–690, 2015.

Ernst SA, Palacios JR, Siegel GJ. Immunocytochemical localization of Na^+,K^+-ATPase catalytic polypeptide in mouse choroid plexus. J Histochem Cytochem 34: 189–195, 1986.

Faber ES, Sah P. Functions of SK channels in central neurons. Clin. Exp. Pharmacol. Physiol. 34 (10): 1077–83, 2007.

Flamion B, Spring KR. Water permeability of apical and basolateral cell membranes of rat inner medullary collecting duct. Am J Physiol. 259:F986-99, 1990.

Garcia-Gonzalo FR, Corbit KC, Sirerol-Piquer MS, Ramaswami G, Otto EA, Noriega TR, Seol AD, Robinson JF, Bennett CL, Josifova DJ, García-Verdugo JM, Katsanis N, Hildebrandt F, Reiter JF. A transition zone complex regulates mammalian ciliogenesis and ciliary membrane composition. Nat Genet. 43(8):776-84, 2011.

Giepmans BN, van Ijzendoorn SC. Epithelial cell-cell junctions and plasma membrane domains. Biochim Biophys Acta. 1788(4):820-31, 2009.

Haas M. The Na-K-Cl cotransporters. Am J Physiol. 267(4 Pt 1):C869-85, 1994.

Halls M, Cooper D. Regulation by Ca^{2+}-Signaling Pathways of Adenylyl Cyclases. Cold Spring Harb Perspect Biol. 3(1): a004143, 2011.

Held D, Fencl V, Pappenheimer JR. Electrical potential of cerebrospinal fluid. J Neurophysiol 27: 942–959, 1964.

Huh MS, Todd Ma Fau - Picketts DJ, Picketts DJ. SCO-ping out the mechanisms underlying the etiology of hydrocephalus. Physiology (Bethesda) 24:117-126, 2009.

Husted RF, Reed DJ. Regulation of cerebrospinal fluid bicarbonate by the cat choroid plexus. J Physiol 267: 411–428, 1977.

Ivan L, Wolfgang L, Michael JS, Miguel AV. TRPV4 channel participates in receptor-operated calcium entry and ciliary beat frequency regulation in mouse airway epithelial cells. Proc Natl Acad Sci U S A. 105(34):12611-6, 2008.

Jafarzadeh F, Field M, Harrington D, Kuduvalli M, Oo A, Kendall J, Desmond M, Mills K. Novel application of acetazolamide to reduce cerebrospinal fluid production in patients undergoing thoracoabdominal aortic surgery. Interact Cardiovasc Thorac Surg. 18(1): 21–26, 2014.

Johanson CE, Duncan JA 3rd, Klinge PM, Brinker T, Stopa EG, Silverberg GD. Multiplicity of cerebrospinal fluid functions: New challenges in health and disease. Cerebrospinal Fluid Res. 14:10, 2008.

Johanson CE, Sweeney SM, Parmelee JT, Epstein MH. Cotransport of sodium and chloride by the adult mammalian choroid plexus. Am J Physiol Cell Physiol 258: C211–C216, 1990.

Kajita H, Omori K, Matsuda H. The chloride channel ClC-2 contributes to the inwardly rectifying Cl^- conductance in cultured porcine choroid plexus epithelial cells. J Physiol 523: 313–324, 2000.

Kao L, Kurtz LM, Shao X, Papadopoulos MC, Liu L, Bok D, Nusinowitz S, Chen B, Stella SL, Andre M, Weinreb J, Luong SS, Piri N, JMK, Newman D, Kurtz I. Severe neurologic impairment in mice with targeted disruption of the electrogenic sodium bicarbonate cotransporter NBCe2 (*Slc4a5* gene). J Biol Chem 286: 32563–32574, 2011.

Keep RF, Xiang J, Betz AL. Potassium cotransport at the rat choroid plexus. Am J Physiol Cell Physiol 267: C1616–C1622, 1994.

Kibble JD, Garner C, Kajita H, Colledge WH, Evans MJ, Radcliff R, Brown PD. Whole cell Cl^- conductances in mouse choroid plexus epithelial cells do not require CFTR expression. Am J Physiol Cell Physiol 272: C1899–C1907, 1997.

Kibble JD, Tresize AO, Brown PD. Properties of the cAMP-activated Cl^- conductance in choroid plexus epithelial cells isolated from the rat. J Physiol 496: 69–80, 1996.

Köhler M, Hirschberg B, Bond CT, Kinzie JM, Marrion NV, Maylie J, Adelman JP. Small-conductance, calcium-activated potassium channels from mammalian brain. Science 273 (5282): 1709–14, 1996.

Kotera T, Brown PD. Two types of potassium current in rat choroid plexus epithelial cells. Pflügers Arch 237: 1994.

Lee EJ, Shina SH, Chunb J, Hyunc S, Kimd Y, Kangae SS. The modulation of TRPV4 channel activity through its Ser 824 residue phosphorylation by SGK1. Animal cells and systems 14(2):99-114, 2010.

Leenen FH. The central role of the brain aldosterone-“ouabain” pathway in saltsensitive hypertension. Biochim Biophys Acta 1802: 1132–1139, 2010.

Loffing J, Kaissling B. Sodium and calcium transport pathways along the mammalian distal nephron: from rabbit to human. Am J Physiol Renal Physiol. 284(4):F628-43, 2003.

Masuzawa T, Ohta T, Kawamura M, Nakahara N, Sato F. Immunohistochemical localization of Na^+-K^+-ATPase in the choroid plexus. Brain Res 302: 357–362, 1984.

Millar ID, Wang S, Brown PD, Barrand MA, Hladky SB. Kv1 and Kir2 potassium channels are expressed in rat brain endothelial cells. Pflugers Arch - Eur J Physiol 456: 379, 2007.

Nimjee SM, Powers CJ, McLendon RE, Grant GA, Fuchs HE. Single-stage bilateral choroid plexectomy for choroid plexus papilloma in a patient presenting with high cerebrospinal fluid output. J Neurosurg Pediatr 5(4):342-5, 2010.

Orlowski J, Grinstein S. Diversity of the mammalian sodium/proton exchanger SLC9 gene family. Pflügers Arch 447: 549–565, 2004.

Ortloff AR, Vio K Fau - Guerra M, Guerra M Fau - Jaramillo K, Jaramillo K Fau - Kaehne T, Kaehne T Fau - Jones H, Jones H Fau - McAllister JP, 2nd, McAllister Jp 2nd Fau - Rodriguez E, Rodriguez E. Role of the subcommissural organ in the pathogenesis of congenital hydrocephalus in the HTx rat. Cell Tissue Res 352:707-725, 2013.

Plant TD, Strotmann R. TRPV4. Handb Exp Pharmacol 179:189–205, 2007.

Plotkin MD, Kaplan MR, Peterson LN, Gullans SR, Hebert SC, Delpire E. Expression of the Na^+-K^+-$2Cl^-$ cotransporter BSC2 in the nervous system. Am J Physiol Cell Physiol 272: C173–C183, 1997.

Pollay M, Hisey B, Reynolds E, Tomkins P, Stevens FA, Smith R. Choroid plexus Na^+/K^+-activated adenosine triphosphatase and cerebrospinal fluid formation. Neurosurgery 17: 768–772, 1985.

Praetorius J, Nejsum LN, Nielsen S. A SLC4A10 gene product maps selectively to the basolateral membrane of choroid plexus epithelial cells. Am J Physiol Cell Physiol 286: C601–C610, 2004.

Praetorius J, Nielsen S. Distribution of sodium transporters and aquaporin-1 in the human choroid plexus. Am J Physiol Cell Physiol 291: C59–C67, 2006.

Quinton PM, Wright EM, Tormey JM. Localization of sodium pumps in the choroid plexus epithelium. J Cell Biol 58: 724–730, 1973.

Reynolds A, Parris A, Evans LA, Lindqvist S, Sharp P, Lewis M, Tighe R, Williams MR. Dynamic and differential regulation of NKCC1 by calcium and cAMP in the native human colonic epithelium. J Physiol. 15;582(Pt 2):507-24, 2007.

Roepke TK, Kanda VA, Purtell K, King EC, Lerner DJ, Abbott GW. KCNE2 forms potassium channels with KCNA3 and KCNQ1 in the choroid plexus epithelium. FASEB J 25: 4264–4273, 2011.

Rosenthal R, Milatz S, Krug SM, Oelrich B, Schulzke JD, Amasheh S, Gunzel D, Fromm M. Claudin-2, a component of the tight junction, forms a paracellular water channel. J Cell Sci 123: 1913–1921, 2010.

Russell JM. Sodium-potassium-chloride cotransport. Physiol Rev 80: 211–276, 2000.

Sang L, Miller JJ, Corbit KC, Giles RH, Brauer MJ, Otto EA, Baye LM, Wen X, Scales SJ, Kwong M, Huntzicker EG, Sfakianos MK, Sandoval W, Bazan JF, Kulkarni P, Garcia-Gonzalo FR, Seol AD, O'Toole JF, Held S, Reutter HM, Lane WS, Rafiq MA, Noor A, Ansar M, Devi AR, Sheffield VC, Slusarski DC, Vincent JB, Doherty DA, Hildebrandt F, Reiter JF, Jackson PK. Mapping the NPHP-JBTS-MKS protein network reveals ciliopathy disease genes and pathways. Cell. 145(4):513-28, 2011.

Sassani P, Pushkin A, Gross E, Gomer A, Abuladze N, Dukkipati R, Carpenito G, Kurtz I. Functional characterization of NBC4: a new electrogenic sodium-bicarbonate cotransporter. Am J Physiol Cell Physiol 282: C408–C416, 2002.

Schroten M, Hanisch FG, Quednau N, Stump C, Riebe R, Lenk M, Wolburg H, Tenenbaum T, Schwerk C. A novel porcine in vitro model of the blood-cerebrospinal fluid barrier with strong barrier function. PLoS One. 7(6):e39835, 2012.

Schwamb R, Dalpiaz A, Miao Y, Gonka J, Khan SA. Clinical manifestations of hydrocephalus: A review. Neurology and Clinical Neuroscience 2:173–177, 2014.

Schwerk C, Papandreou T, Schuhmann D, Nickol L, Borkowski J, Steinmann U, Quednau N, Stump C, Weiss C, Berger J, Wolburg H, Claus H, Vogel U, Ishikawa H, Tenenbaum T, Schroten H. Polar invasion and translocation of *Neisseria meningitidis* and *Streptococcus suis* in a novel human model of the blood-cerebrospinal fluid barrier. PLoS One 7(1):e30069, 2012.

Shibasaki K, Suzuki M, Mizuno A, Tominaga M. Effects of Body Temperature on Neural Activity in the Hippocampus: Regulation of Resting Membrane Potentials by Transient Receptor Potential Vanilloid 4. Journal of Neurosci. 27(7): 1566-1575, 2007.

Siegel GJ, Holm C, Schreiber JH, Desmond T, Ernst SA. Purification of mouse brain Na^+,K^+-ATPase catalytic unit, characterization of antiserum, and immunocytochemical localization in cerebellum, choroid plexus, and kidney. J Histochem Cytochem 32: 1309–1318, 1984.

Smith UM, Consugar M, Tee LJ, McKee BM, Maina EN, Whelan S, Morgan NV, Goranson E, Gissen P, Lilliquist S, Aligianis IA, Ward CJ, Pasha S, Punyashthiti R, Malik Sharif S, Batman PA, Bennett CP, Woods CG, McKeown C, Bucourt M, Miller CA, Cox P, Algazali L, Trembath RC, Torres VE, Attie-Bitach T, Kelly DA, Maher ER, Gattone VH 2nd, Harris PC, Johnson CA. The transmembrane protein meckelin (MKS3) is mutated in Meckel-Gruber syndrome and the wpk rat. Nat Genet. 38(2):191-6, 2006.

Song MY, Yuan JX. Introduction to TRP channels: structure, function, and regulation. Adv Exp Med Biol. 661:99-108, 2010.

Stackman RW, Hammond RS, Linardatos E, Gerlach A, Maylie J, Adelman JP, Tzounopoulos T. Small conductance Ca^{2+}-activated K^+ channels modulate synaptic plasticity and memory encoding. J. Neurosci. 22 (23): 10163–71, 2002.

Sung S, Eun L, Jaesun C, Sunghee H, Sang K. Phosphorylation on TRPV4 serine 824 regulates interaction with STIM1. Open Biochem J. 9:24-33, 2015.
Takayama Y, Shibasaki K, Suzuki Y, Yamanaka A, Tominaga M. Modulation of water efflux through functional interaction between TRPV4 and TMEM16A/anoctamin 1. FASEB J. 28(5):2238-48, 2014.

Tyerman DS. Nonselective cation channels. Multiple functions and commonalities. Plant Physiology 128(2): 327-328, 2002.

Van Huysse JW, Amin MS, Yang B, Leenen FH. Salt-induced hypertension in a mouse model of Liddle syndrome is mediated by epithelial sodium channels in the brain. Hypertension 60: 691–696, 2012.

Venkatachalam K, Montell C. TRP channels. Annu Rev Biochem. 76:387-417, 2007.

Virkki LV, Wilson DA, Vaughan-Jones RD, Boron WF. Functional characterization of human NBC4 as an electrogenic Na^+-HCO_3^- cotransporter (NBCe2). Am J Physiol Cell Physiol 282: C1278–C1289, 2002.

Vogh BP, Godman DR, Maren TH. Effect of AlCl3 and other acids on cerebrospinal fluid production: a correction. J Pharmacol Exp Ther. 243(1):35-9, 1987.

Wang HW, Amin MS, El-Shahat E, Huang BS, Tuana BS, Leenen FH. Effects of central sodium on epithelial sodium channels in rat brain. Am J Physiol Regul Integr Comp Physiol 299: R222–R233, 2010.

Webster MK, Goya L, Ge Y, Maiyar AC, Firestone GL. Characterization of sgk, a novel member of the serine/threonine protein kinase gene family which is transcriptionally induced by glucocorticoids and serum. Molecular and Cellular Biology 13 (4): 2031–40, 1993.

Welch K, Sadler K. Electrical potentials of choroid plexus of the rabbit. J Neurosurg 22: 344–351, 1965.

Welch K. Secretion of cerebrospinal fluid by choroid plexus of the rabbit. Am J Physiol 205: 617–624, 1963.

Whittembury G, Paz-Aliaga A, Biondi A, Carpi-Medina P, Gonzalez E, Linares H. Pathways for volume flow and volume regulation in leaky epithelia. Pflügers Arch 405 Suppl 1: S17–S22, 1985.

Will C, Fromm M, Muller D. Claudin tight junction proteins: novel aspects in paracellular transport. Perit Dial Int 28: 577–584, 2008.

Wright EM. Transport processes in the formation of the cerebrospinal fluid. Rev Physiol Biochem Pharmacol 83: 3–34, 1978.

Wu Q, Delpire E, Hebert SC, Strange K. Functional demonstration of Na-K-2Cl cotransporter activity in isolated, polarized choroid plexus cells. Am J Physiol Cell Physiol 275: C1565–C1572, 1998.

Yadav, Yad R, Parihar, Vijay, Sinha, Mallika. Lumbar peritoneal shunt. Neurology India 58 (2): 179–84, 2010.

Yingst DR. Modulation of the Sodium-Potassium-ATPase by calcium and intracellular proteins. Annu Rev Physiol. 50:291-303, 1988.

Zheng W, Zhao Q. Establishment and characterization of an immortalized Z310 choroidal epithelial cell line from murine choroid plexus. Brain Res. 958(2): 371–380, 2002.

Zhou Y, Lingle CJ. Paxilline inhibits BK channels by an almost exclusively closed-channel block mechanism. J Gen Physiol. 144(5):415-40, 2014.

FIGURES

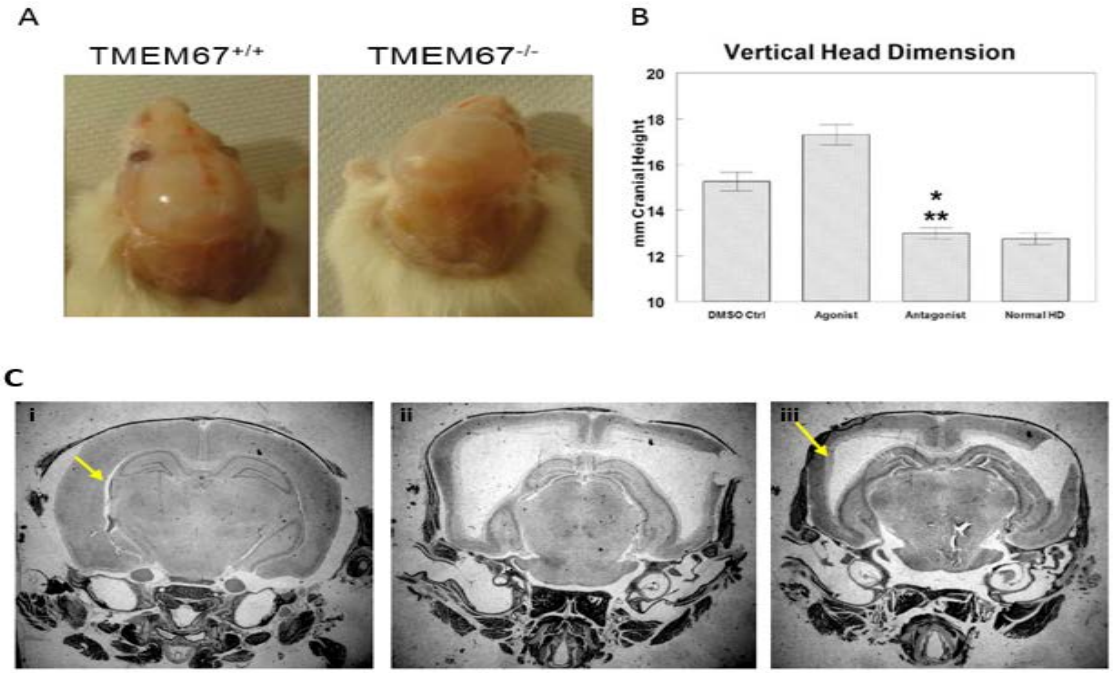

Figure 1.1: Effect of TRPV4 modulators on vertical size and head dimension in the Wpk rat model. (A) Heads of 17 day old wild type animals (TMEM67$^{+/+}$) and homozygous affected animals (TMEM67$^{-/-}$). (B) Bar graph of vertical head dimension of animals treated with DMSO control, agonist (GSK1016797, 0.003mg/kg body weight) and antagonist (HC067047, 0.03mg/kg) are all affected animals while normal indicates the normal littermates from day 8 to 17. Antagonist treatment limited cranial enlargement (Mean ± SEM, * = <0.01 difference from DMSO control, **= <0.001 difference from TRPV4 agonist). (C) Histological section of H&E stained brains from PD17 rats. The light area (yellow arrows) indicates the fluid that forms the normal ventricles (i) as compared to the fluid in a PD17 hydrocephalic Wpk/Wpk animal (ii). (iii) shows decreased ventricle size due to the antagonist treatment.

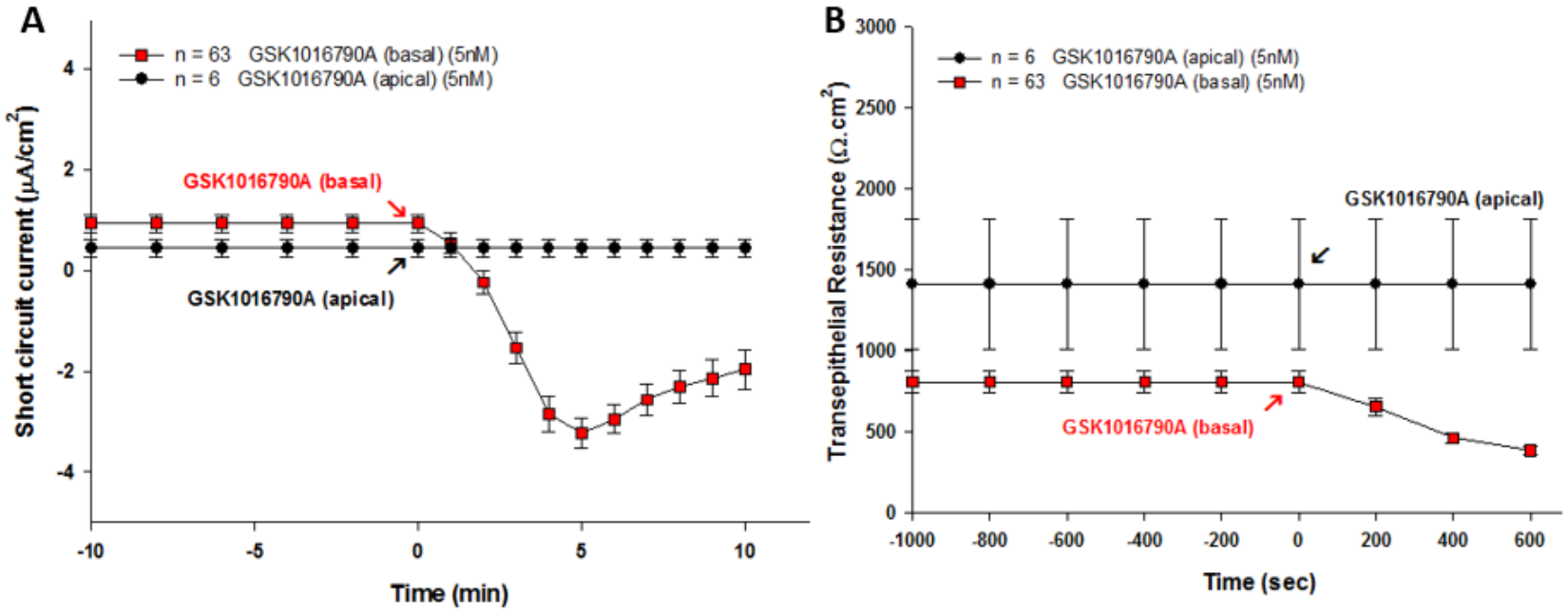

Figure 3.1: Effect of TRPV4 agonists on confluent cultures of PCP-R. PCP-R cells were grown on permeable Transwell membranes for 10 to 12 days to reach confluence, excised, mounted in an Ussing chamber, and allowed to develop a stable basal short-circuit current (SCC). SCC is a measure of net transepithelial ion transport. (A) SCC plots. After stabilization, GSK1016790A (5nM) was added to the apical or basal bathing media (time, t= 0) The symbols denote the means of 6 or 63 experiments ± SE. (B) TER plots: 2mV pulses were induced every 200 seconds and the current displacement during the pulse was used to calculate the transepithelial resistance via Ohm's law. After stabilization, GSK1016790A (5nM) was added to the apical or basal bathing media (time, t= 0). The symbols denote the means of 6 or 63 experiments ± SE.

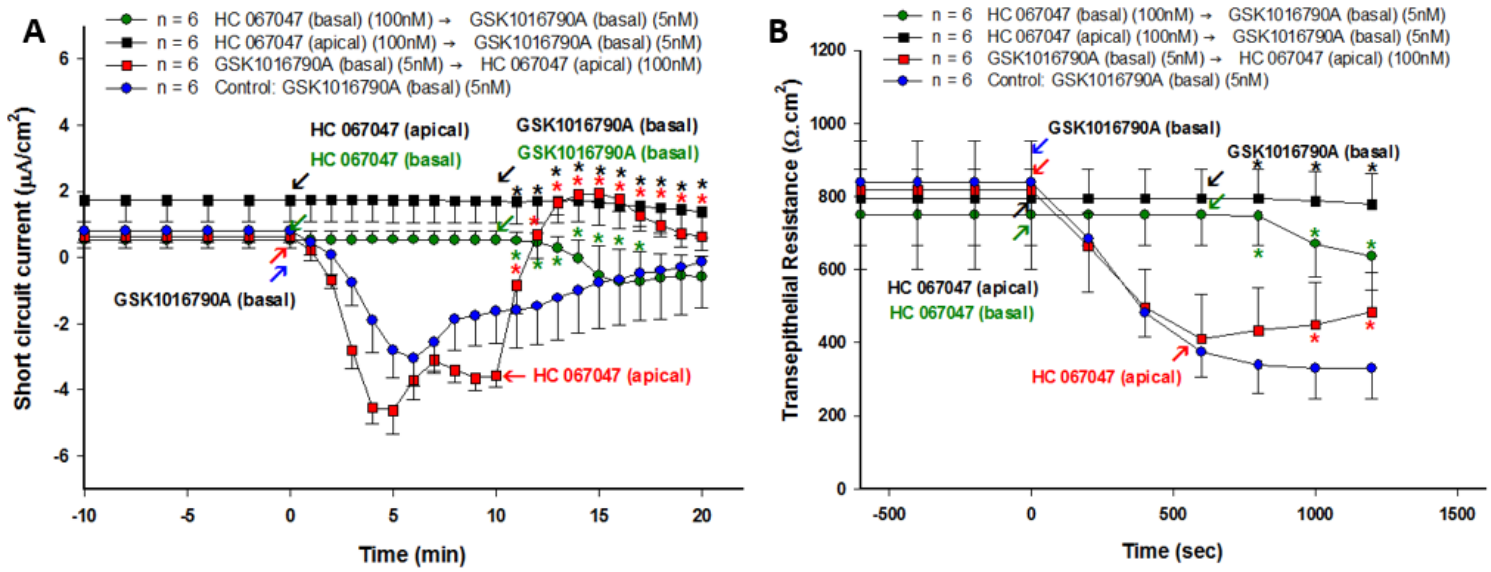

Figure 3.2: GSK1016790A mediated ion flux and TER decline is TRPV4 specific. PCP-R cells were grown on permeable Transwell membranes for 10 to 12 days to reach confluence, excised, mounted in an Ussing chamber, and allowed to develop a stable basal short-circuit current (SCC). SCC is a measure of net transepithelial ion transport. (A) SCC plots: After stabilization, HC067047 (100nM) or GSK1016790A (5 nM) were added either to the apical or basal bathing media (time, t = 0 or 10). The symbols denote the means of 6 experiments ± SE. Blue line represents the control experiment where only GSK1016790A (5nM) was added to the basal bathing media (time, t= 0). The symbols denote the means of 6 experiments ± SE. (*) denotes statistically significant SCC change compared to the control experiments ($p \leq 0.05$; Student's t-test). (B) TER plots: 2mV pulses were induced every 200 seconds and the current displacement during the pulse was used to calculate the transepithelial resistance via Ohm's law. After stabilization, HC067047 (100nM) or GSK1016790A (5 nM) were added either to the apical or basal bathing media (time, t = 0 or 10). The symbols denote the means of 6 experiments ± SE. Blue line represents the control experiment where only GSK1016790A (5nM) was added to the basal bathing media (time, t= 0). The symbols denote the means of 6 experiments ± SE. (*) denotes statistically significant TER change compared to the control experiments ($p \leq 0.05$; Student's t-test).

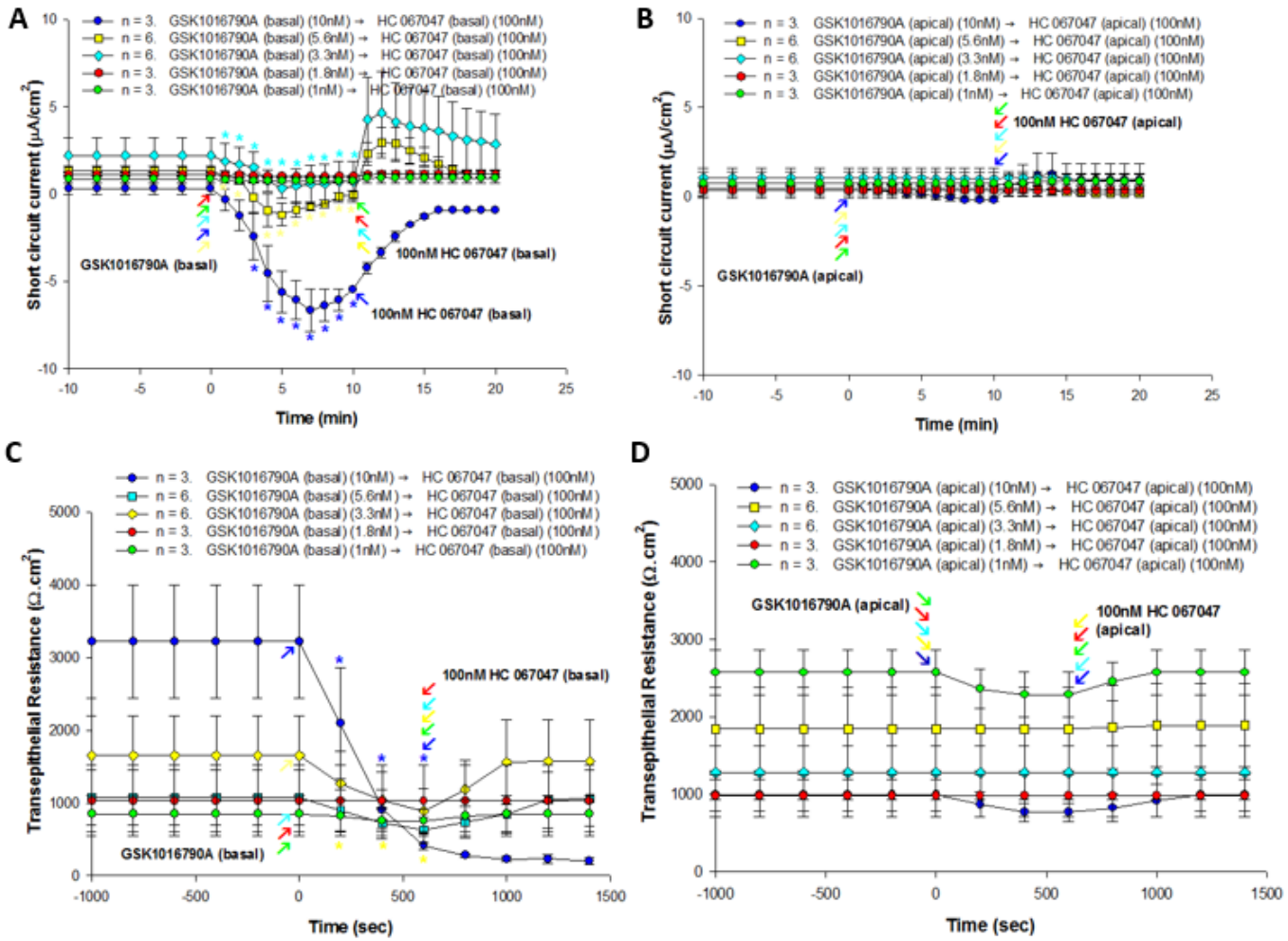
A
n = 3. GSK1016790A (basal) (10nM) → HC 067047 (basal) (100nM)
n = 6. GSK1016790A (basal) (5.6nM) → HC 067047 (basal) (100nM)
n = 6. GSK1016790A (basal) (3.3nM) → HC 067047 (basal) (100nM)
n = 3. GSK1016790A (basal) (1.8nM) → HC 067047 (basal) (100nM)
n = 3. GSK1016790A (basal) (1nM) → HC 067047 (basal) (100nM)
Short circuit current (μA/cm²)
GSK1016790A (basal)
100nM HC 067047 (basal)
100nM HC 067047 (basal)
Time (min)
B
n = 3. GSK1016790A (apical) (10nM) → HC 067047 (apical) (100nM)
n = 6. GSK1016790A (apical) (5.6nM) → HC 067047 (apical) (100nM)
n = 6. GSK1016790A (apical) (3.3nM) → HC 067047 (apical) (100nM)
n = 3. GSK1016790A (apical) (1.8nM) → HC 067047 (apical) (100nM)
n = 3. GSK1016790A (apical) (1nM) → HC 067047 (apical) (100nM)
Short circuit current (μA/cm²)
100nM HC 067047 (apical)
GSK1016790A (apical)
Time (min)
C
n = 3. GSK1016790A (basal) (10nM) → HC 067047 (basal) (100nM)
n = 6. GSK1016790A (basal) (5.6nM) → HC 067047 (basal) (100nM)
n = 6. GSK1016790A (basal) (3.3nM) → HC 067047 (basal) (100nM)
n = 3. GSK1016790A (basal) (1.8nM) → HC 067047 (basal) (100nM)
n = 3. GSK1016790A (basal) (1nM) → HC 067047 (basal) (100nM)
Transepithelial Resistance (Ω.cm²)
100nM HC 067047 (basal)
GSK1016790A (basal)
Time (sec)
D
n = 3. GSK1016790A (apical) (10nM) → HC 067047 (apical) (100nM)
n = 6. GSK1016790A (apical) (5.6nM) → HC 067047 (apical) (100nM)
n = 6. GSK1016790A (apical) (3.3nM) → HC 067047 (apical) (100nM)
n = 3. GSK1016790A (apical) (1.8nM) → HC 067047 (apical) (100nM)
n = 3. GSK1016790A (apical) (1nM) → HC 067047 (apical) (100nM)
Transepithelial Resistance (Ω.cm²)
GSK1016790A (apical)
100nM HC 067047 (apical)
Time (sec)

Figure 3.3

Figure 3.3: TRPV4 agonist dose response. PCP-R cells were grown on permeable Transwell membranes for 10 to 12 days to reach confluence, excised, mounted in an Ussing chamber, and allowed to develop a stable basal short-circuit current (SCC). SCC is a measure of net transepithelial ion transport. (A) SCC plots: After stabilization, 1nM, 1.8nM, 3.3nM, 5.6nM or 10nM GSK1016790A (agonist) was added to the basal bathing media (time, t = 0) and HC067047 (antagonist) (100 nM) was added to the basal bathing media (time, t=10). The symbols denote the means of 3 or 6 experiments ± SE. 1nM plot was used as the control. (*) denotes statistically significant SCC change compared to the control experiments ($p \leq 0.05$; Student's t-test). (B) SCC plots: After stabilization, 1nM, 1.8nM, 3.3nM, 5.6nM or 10nM GSK1016790A (agonist) was added to the apical bathing media (time, t = 0) and HC067047 (antagonist) (100 nM) was added to the apical bathing media (time, t=10). The symbols denote the means of 3 or 6 experiments ± SE. 1nM plot was used as the control. 2mV pulses were induced every 200 seconds and the current displacement during the pulse was used to calculate the transepithelial resistance via Ohm's law. (C) TER plots: After stabilization, 1nM, 1.8nM, 3.3nM, 5.6nM or 10nM GSK1016790A (agonist) was added to the basal bathing media (time, t = 0) and HC067047 (antagonist) (100 nM) was added to the basal bathing media (time, t=600). The symbols denote the means of 3 or 6 experiments ± SE. 1nM plot was used as a control. (*) denotes statistically significant TER change compared to the control experiments ($p \leq 0.05$; Student's t-test). (D) TER plots: After stabilization, 1nM, 1.8nM, 3.3nM, 5.6nM or 10nM GSK1016790A (agonist) was added to the apical bathing media (time, t = 0) and HC067047 (antagonist) (100 nM) was added to the apical bathing media (time, t=600). The symbols denote the means of 3 or 6 experiments ± SE.

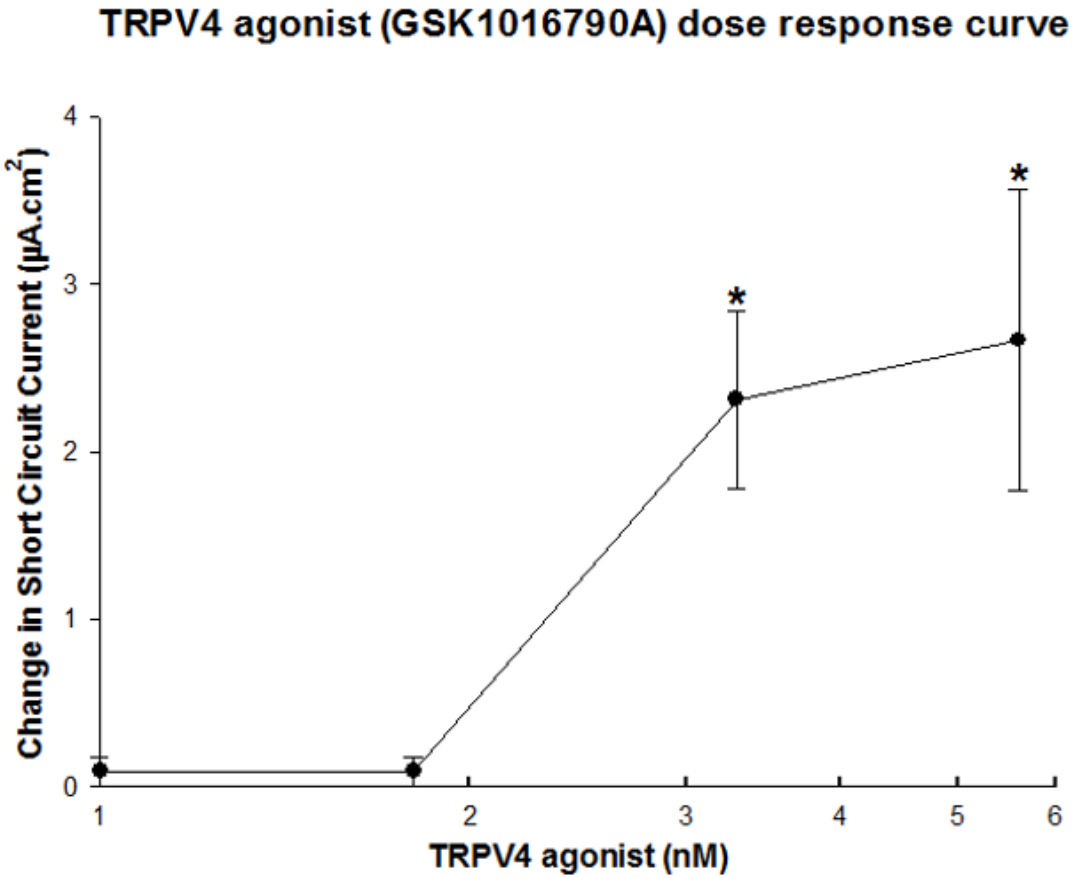

Figure 3.4: TRPV4 agonist dose response curve. PCP-R cells were grown on permeable Transwell membranes for 10 to 12 days to reach confluence, excised, mounted in an Ussing chamber, and allowed to develop a stable basal short-circuit current (SCC). SCC is a measure of net transepithelial ion transport. n (1nM) = 3. n (1.8nM) = 3. n (3.3nM) = 6. n (5.6nM) = 6. 1nM plot was used as the control. (*) denotes statistically significant SCC change compared to the control experiments ($p \leq 0.05$; Student's t-test).

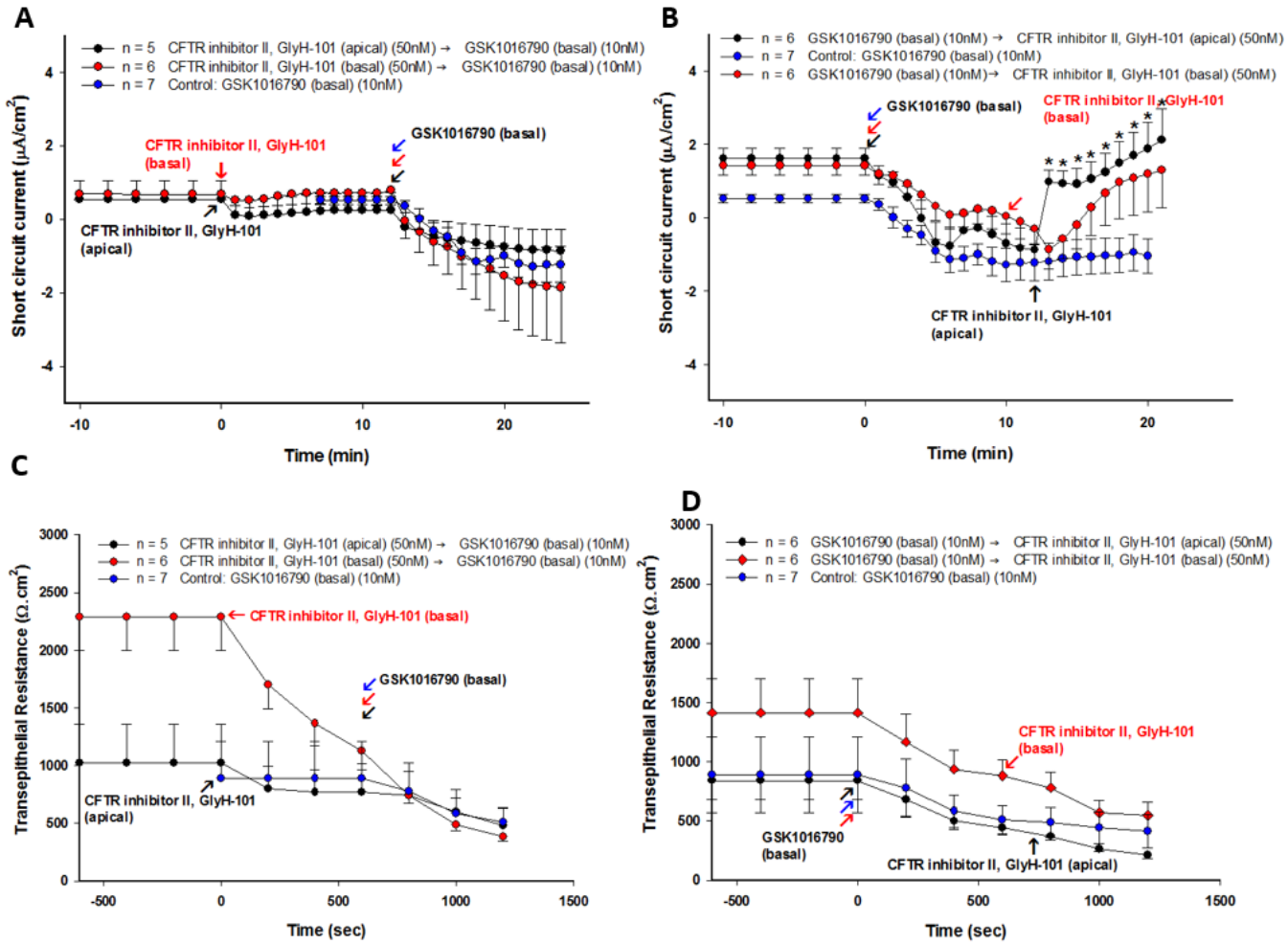
A
n = 5 CFTR inhibitor II, GlyH-101 (apical) (50nM) → GSK1016790 (basal) (10nM)
n = 6 CFTR inhibitor II, GlyH-101 (basal) (50nM) → GSK1016790 (basal) (10nM)
n = 7 Control: GSK1016790 (basal) (10nM)
CFTR inhibitor II, GlyH-101 (basal)
GSK1016790 (basal)
CFTR inhibitor II, GlyH-101 (apical)
Short circuit current (μA/cm²)
Time (min)
B
n = 6 GSK1016790 (basal) (10nM) → CFTR inhibitor II, GlyH-101 (apical) (50nM)
n = 7 Control: GSK1016790 (basal) (10nM)
n = 6 GSK1016790 (basal) (10nM)→ CFTR inhibitor II, GlyH-101 (basal) (50nM)
GSK1016790 (basal)
CFTR inhibitor II, GlyH-101 (basal)
CFTR inhibitor II, GlyH-101 (apical)
Short circuit current (μA/cm²)
Time (min)
C
n = 5 CFTR inhibitor II, GlyH-101 (apical) (50nM) → GSK1016790 (basal) (10nM)
n = 6 CFTR inhibitor II, GlyH-101 (basal) (50nM) → GSK1016790 (basal) (10nM)
n = 7 Control: GSK1016790 (basal) (10nM)
CFTR inhibitor II, GlyH-101 (basal)
GSK1016790 (basal)
CFTR inhibitor II, GlyH-101 (apical)
Transepithelial Resistance (Ω.cm²)
Time (sec)
D
n = 6 GSK1016790 (basal) (10nM) → CFTR inhibitor II, GlyH-101 (apical) (50nM)
n = 6 GSK1016790 (basal) (10nM) → CFTR inhibitor II, GlyH-101 (basal) (50nM)
n = 7 Control: GSK1016790 (basal) (10nM)
CFTR inhibitor II, GlyH-101 (basal)
GSK1016790 (basal)
CFTR inhibitor II, GlyH-101 (apical)
Transepithelial Resistance (Ω.cm²)
Time (sec)

Figure 3.5

Figure 3.5: TRPV4 mediated ion flux activates CFTR in the basolateral membrane and is accompanied by a decrease in TER. PCP-R cells were grown on permeable Transwell membranes for 10 to 12 days to reach confluence, excised, mounted in an Ussing chamber, and allowed to develop a stable basal short-circuit current (SCC). SCC is a measure of net transepithelial ion transport. (A) SCC plots: After stabilization, CFTR inhibitor II, GlyH-101 (50nM) was added either to the apical or basal bathing media (time, t= 0) and GSK1016790A (10nM) was added to the basal bathing media (time, t= 12). The symbols denote the means of 5 or 6 experiments ± SE. Blue line represents the control experiment where only GSK1016790A (10nM) was added to the basal bathing media (time, t= 12). The symbols denote the means of 7 experiments ± SE. (B) SCC plots: After stabilization, GSK1016790A (10nM) was added to the basal bathing media (time, t= 0) and CFTR inhibitor II, GlyH-101 (50nM) was added either to the apical or basal bathing media (time, t= 12). The symbols denote the means of 6 experiments ± SE. Blue line represents the control experiment where only GSK1016790A (10nM) was added to the basal bathing media (time, t= 0). The symbols denote the means of 7 experiments ± SE. (*) denotes statistically significant SCC change compared to the control experiments ($p \leq 0.05$; Student's t-test). 2mV pulses were induced every 200 seconds and the current displacement during the pulse was used to calculate the transepithelial resistance via Ohm's law. (C) TER plots: After stabilization, CFTR inhibitor II, GlyH-101 (50nM) was added either to the apical or basal bathing media (time, t= 0) and GSK1016790A (10nM) was added to the basal bathing media (time, t= 720). The symbols denote the means of 5 or 6 experiments ± SE. Blue line represents the control experiment where only GSK1016790A (10nM) was added to the basal bathing media (time, t= 720). The symbols denote the means of 7 experiments ± SE. (D) TER plots: After stabilization, GSK1016790A (10nM) was added to the basal bathing media (time, t= 0) and CFTR inhibitor II, GlyH-101 (50nM) was added either to the apical or basal bathing media (time, t= 720). The symbols denote the means of 6 experiments ± SE. Blue line represents the control experiment where only GSK1016790A (10nM) was added to the basal bathing media (time, t= 0). The symbols denote the means of 7 experiments ± SE.

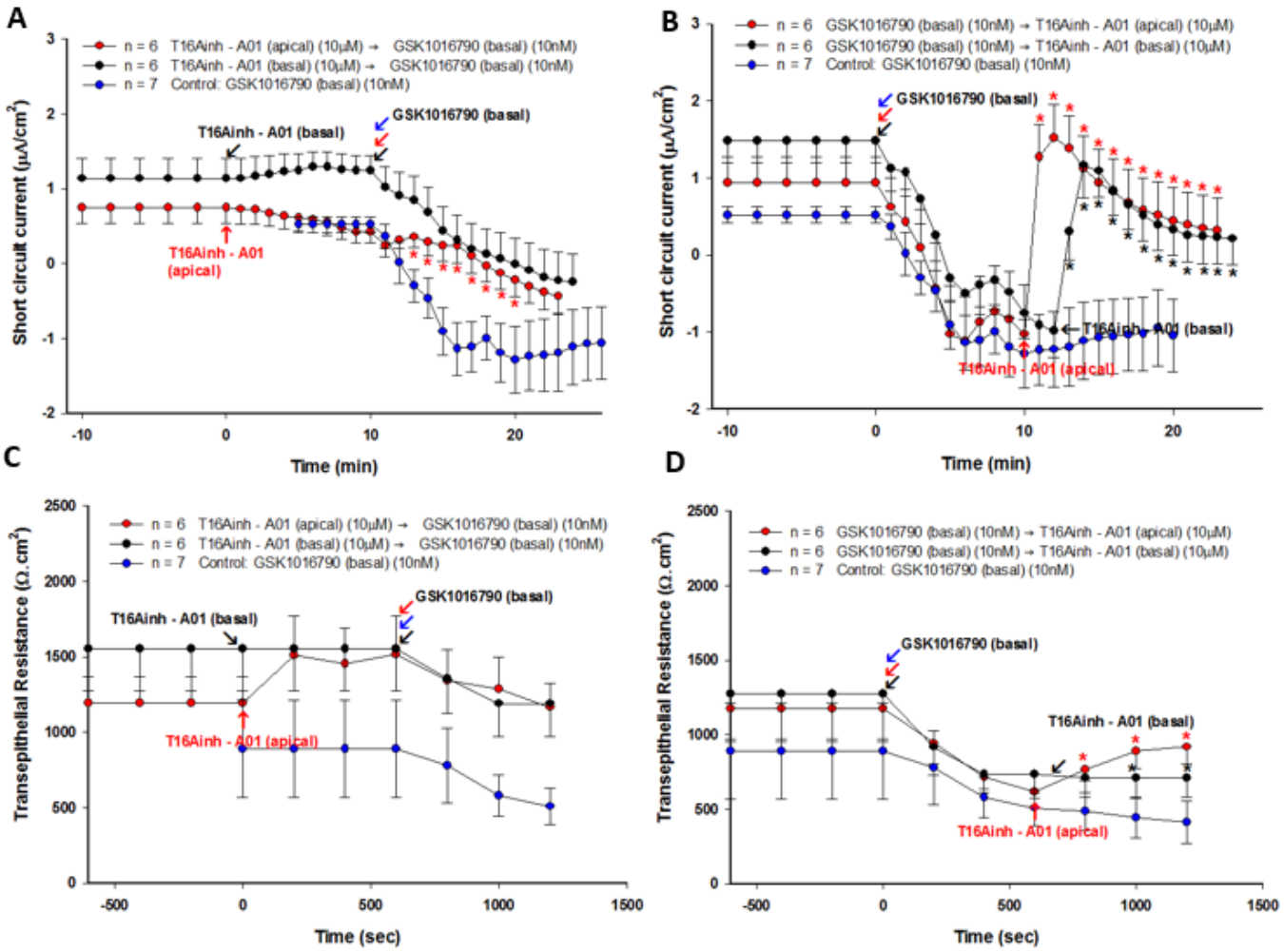
A
n = 6 T16Ainh - A01 (apical) (10μM) → GSK1016790 (basal) (10nM)
n = 6 T16Ainh - A01 (basal) (10μM) → GSK1016790 (basal) (10nM)
n = 7 Control: GSK1016790 (basal) (10nM)
Short circuit current (μA/cm²)
T16Ainh - A01 (basal)
GSK1016790 (basal)
T16Ainh - A01 (apical)
Time (min)
B
n = 6 GSK1016790 (basal) (10nM) → T16Ainh - A01 (apical) (10μM)
n = 6 GSK1016790 (basal) (10nM) → T16Ainh - A01 (basal) (10μM)
n = 7 Control: GSK1016790 (basal) (10nM)
Short circuit current (μA/cm²)
GSK1016790 (basal)
T16Ainh - A01 (basal)
T16Ainh - A01 (apical)
Time (min)
C
n = 6 T16Ainh - A01 (apical) (10μM) → GSK1016790 (basal) (10nM)
n = 6 T16Ainh - A01 (basal) (10μM) → GSK1016790 (basal) (10nM)
n = 7 Control: GSK1016790 (basal) (10nM)
Transepithelial Resistance (Ω.cm²)
T16Ainh - A01 (basal)
GSK1016790 (basal)
T16Ainh - A01 (apical)
Time (sec)
D
n = 6 GSK1016790 (basal) (10nM) → T16Ainh - A01 (apical) (10μM)
n = 6 GSK1016790 (basal) (10nM) → T16Ainh - A01 (basal) (10μM)
n = 7 Control: GSK1016790 (basal) (10nM)
Transepithelial Resistance (Ω.cm²)
GSK1016790 (basal)
T16Ainh - A01 (basal)
T16Ainh - A01 (apical)
Time (sec)

Figure 3.6

Figure 3.6: TRPV4 mediated ion flux activates TMEM16A in the basal membrane and is accompanied by a reversal in TER change. PCP-R cells were grown on permeable Transwell membranes for 10 to 12 days to reach confluence, excised, mounted in an Ussing chamber, and allowed to develop a stable basal short-circuit current (SCC). SCC is a measure of net transepithelial ion transport. (A) SCC plots: After stabilization, T16Ainh – A01 (10µM) was added either to the basal or apical bathing media (time, t= 0) and GSK1016790A (10nM) was added to the basal bathing media (time, t= 10). The symbols denote the means of 6 experiments ± SE. Blue line represents the control experiment where only GSK1016790A (10nM) was added to the basal bathing media (time, t= 10). The symbols denote the means of 7 experiments ± SE. (*) denotes statistically significant SCC change compared to the control experiments ($p \leq 0.05$; Student's t-test). (B) SCC plots: After stabilization, GSK1016790A (10nM) was added to the basal bathing media (time, t= 0) and T16Ainh – A01 (10µM) was added either to the apical or basal bathing media (time, t= 12). The symbols denote the means of 6 experiments ± SE. Blue line represents the control experiment where only GSK1016790A (10nM) was added to the basal bathing media (time, t= 0). The symbols denote the means of 7 experiments ± SE. (*) denotes statistically significant SCC change compared to the control experiments ($p \leq 0.05$; Student's t-test). 2mV pulses were induced every 200 seconds and the current displacement during the pulse was used to calculate the transepithelial resistance via Ohm's law. (C) TER plots: After stabilization, T16Ainh – A01 (10µM) was added either to the apical or basal bathing media (time, t= 0) and GSK1016790A (10nM) was added to the basal bathing media (time, t= 600). The symbols denote the means of 6 experiments ± SE. Blue line represents the control experiment where only GSK1016790A (10nM) was added to the basal bathing media (time, t= 600). The symbols denote the means of 7 experiments ± SE. (D) TER plots: After stabilization, GSK1016790A (10nM) was added to the basal bathing media (time, t= 0) and T16Ainh – A01 (10µM) was added either to the apical or basal bathing media (time, t= 720). The symbols denote the means of 6 experiments ± SE. Blue line represents the control experiment where only GSK1016790A (10nM) was added to the basal bathing media (time, t= 0). The symbols denote the means of 7 experiments ± SE. (*) denotes statistically significant TER change compared to the control experiments ($p \leq 0.05$; Student's t-test).

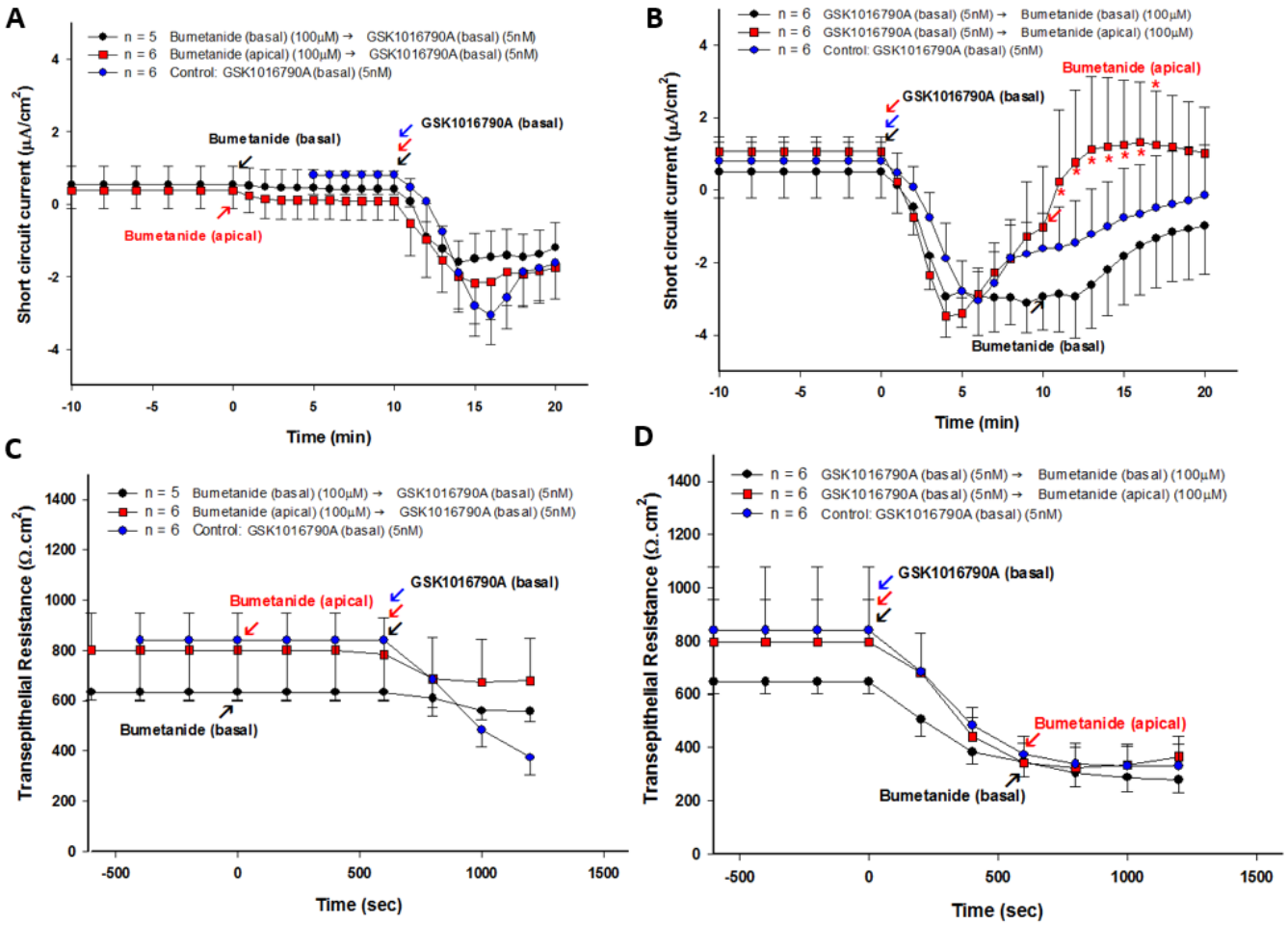
A
n = 5 Bumetanide (basal) (100μM) → GSK1016790A (basal) (5nM)
n = 6 Bumetanide (apical) (100μM) → GSK1016790A (basal) (5nM)
n = 6 Control: GSK1016790A (basal) (5nM)
Bumetanide (basal)
GSK1016790A (basal)
Bumetanide (apical)
Short circuit current (μA/cm²)
Time (min)
B
n = 6 GSK1016790A (basal) (5nM) → Bumetanide (basal) (100μM)
n = 6 GSK1016790A (basal) (5nM) → Bumetanide (apical) (100μM)
n = 6 Control: GSK1016790A (basal) (5nM)
Bumetanide (apical)
GSK1016790A (basal)
Bumetanide (basal)
Short circuit current (μA/cm²)
Time (min)
C
n = 5 Bumetanide (basal) (100μM) → GSK1016790A (basal) (5nM)
n = 6 Bumetanide (apical) (100μM) → GSK1016790A (basal) (5nM)
n = 6 Control: GSK1016790A (basal) (5nM)
Bumetanide (apical)
GSK1016790A (basal)
Bumetanide (basal)
Transepithelial Resistance (Ω.cm²)
Time (sec)
D
n = 6 GSK1016790A (basal) (5nM) → Bumetanide (basal) (100μM)
n = 6 GSK1016790A (basal) (5nM) → Bumetanide (apical) (100μM)
n = 6 Control: GSK1016790A (basal) (5nM)
GSK1016790A (basal)
Bumetanide (apical)
Bumetanide (basal)
Transepithelial Resistance (Ω.cm²)
Time (sec)

Figure 3.7

Figure 3.7: NKCC1 is apical in PCP-R. PCP-R cells were grown on permeable Transwell membranes for 10 to 12 days to reach confluence, excised, mounted in an Ussing chamber, and allowed to develop a stable basal short-circuit current (SCC). SCC is a measure of net transepithelial ion transport. (A) SCC plots: After stabilization, bumetanide (100µM) was added either to the apical or basal bathing media (time, t= 0) and GSK1016790A (5nM) was added to the basal bathing media (time, t= 10). The symbols denote the means of 5 or 6 experiments ± SE. Blue line represents the control experiment where only GSK1016790A (5nM) was added to the basal bathing media (time, t= 10). The symbols denote the means of 6 experiments ± SE. (B) SCC plots: After stabilization, GSK1016790A (5nM) was added to the basal bathing media (time, t= 0) and bumetanide (100µM) was added either to the apical or basal bathing media (time, t= 10). The symbols denote the means of 6 experiments ± SE. Blue line represents the control experiment where only GSK1016790A (5nM) was added to the basal bathing media (time, t= 0). The symbols denote the means of 6 experiments ± SE. (*) denotes statistically significant SCC change compared to the control experiments ($p \leq 0.05$; Student's t-test). 2mV pulses were induced every 200 seconds and the current displacement during the pulse was used to calculate the transepithelial resistance via Ohm's law. (C) TER plots: After stabilization, bumetanide (100µM) was added either to the basal bathing media (time, t= 0) and GSK1016790A (5nM) was added to the basal bathing media (time, t= 600). The symbols denote the means of 5 or 6 experiments ± SE. Blue line represents the control experiment where only GSK1016790A (5nM) was added to the basal bathing media (time, t= 600). The symbols denote the means of 6 experiments ± SE. (D) TER plots: After stabilization, GSK1016790A (5nM) was added to the basal bathing media (time, t= 0) and bumetanide (100µM) was added either to the apical or basal bathing media (time, t= 600). The symbols denote the means of 6 experiments ± SE. Blue line represents the control experiment where only GSK1016790A (5nM) was added to the basal bathing media (time, t= 0). The symbols denote the means of 6 experiments ± SE.

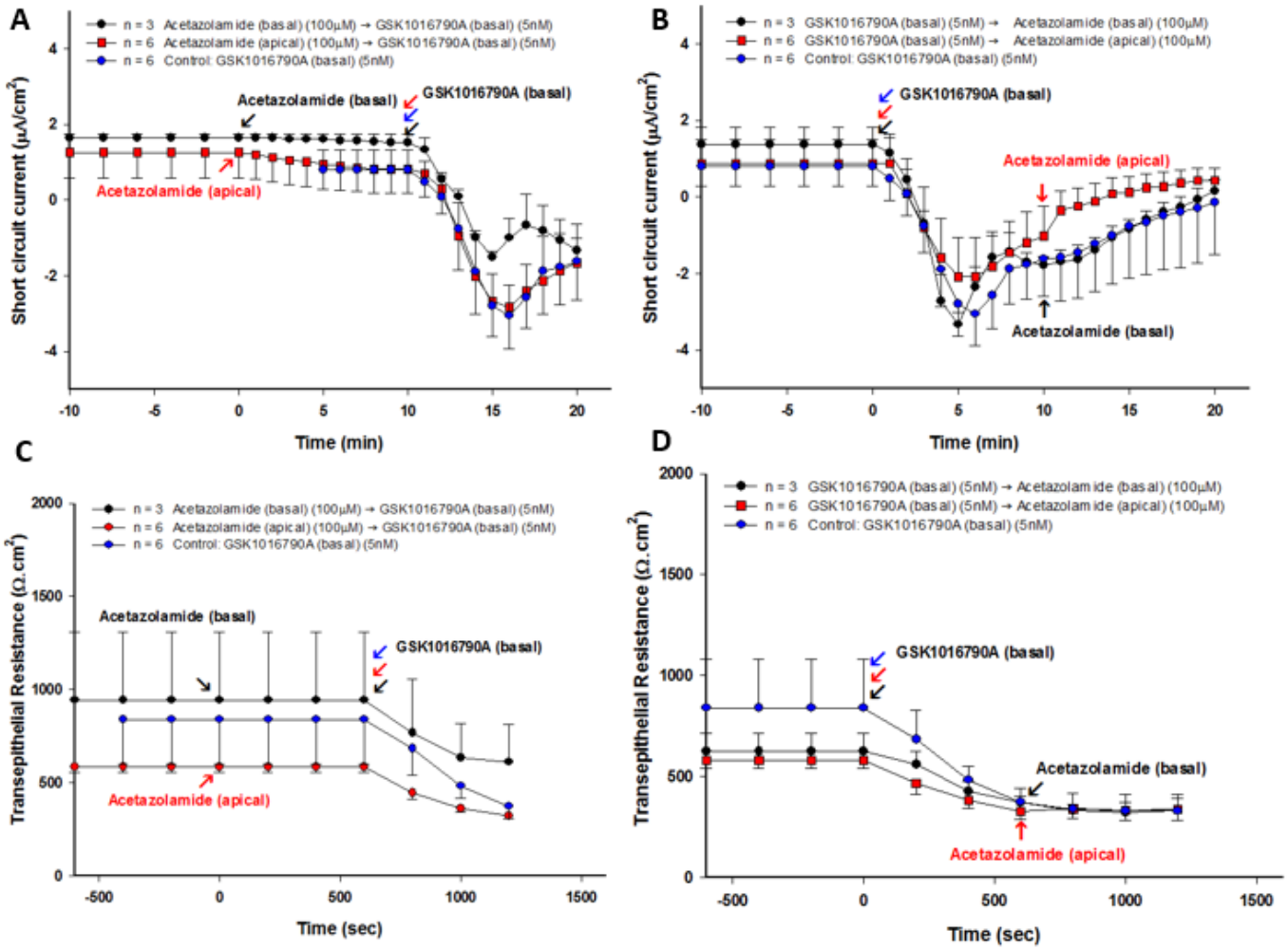
A
n = 3 Acetazolamide (basal) (100µM) → GSK1016790A (basal) (5nM)
n = 6 Acetazolamide (apical) (100µM) → GSK1016790A (basal) (5nM)
n = 6 Control: GSK1016790A (basal) (5nM)
Acetazolamide (basal)
GSK1016790A (basal)
Acetazolamide (apical)
Short circuit current (µA/cm²)
Time (min)
B
n = 3 GSK1016790A (basal) (5nM) → Acetazolamide (basal) (100µM)
n = 6 GSK1016790A (basal) (5nM) → Acetazolamide (apical) (100µM)
n = 6 Control: GSK1016790A (basal) (5nM)
GSK1016790A (basal)
Acetazolamide (apical)
Acetazolamide (basal)
Short circuit current (µA/cm²)
Time (min)
C
n = 3 Acetazolamide (basal) (100µM) → GSK1016790A (basal) (5nM)
n = 6 Acetazolamide (apical) (100µM) → GSK1016790A (basal) (5nM)
n = 6 Control: GSK1016790A (basal) (5nM)
Acetazolamide (basal)
GSK1016790A (basal)
Acetazolamide (apical)
Transepithelial Resistance (Ω.cm²)
Time (sec)
D
n = 3 GSK1016790A (basal) (5nM) → Acetazolamide (basal) (100µM)
n = 6 GSK1016790A (basal) (5nM) → Acetazolamide (apical) (100µM)
n = 6 Control: GSK1016790A (basal) (5nM)
GSK1016790A (basal)
Acetazolamide (basal)
Acetazolamide (apical)
Transepithelial Resistance (Ω.cm²)
Time (sec)

Figure 3.8

Figure 3.8: TRPV4 mediated ion flux and TER decline is not effected by acetazolamide. PCP-R cells were grown on permeable Transwell membranes for 10 to 12 days to reach confluence, excised, mounted in an Ussing chamber, and allowed to develop a stable basal short-circuit current (SCC). SCC is a measure of net transepithelial ion transport. (A) SCC plots: After stabilization, acetazolamide (100µM) was added either to the apical or basal bathing media (time, t= 0) and GSK1016790A (5nM) was added to the basal bathing media (time, t= 10). The symbols denote the means of 6 experiments ± SE. Blue line represents the control experiment where only GSK1016790A (5nM) was added to the basal bathing media (time, t= 10). The symbols denote the means of 6 experiments ± SE. (B) SCC plots: After stabilization, GSK1016790A (5nM) was added to the basal bathing media (time, t= 0) and acetazolamide (100µM) was added either to the apical or basal bathing media (time, t= 10). The symbols denote the means of 6 experiments ± SE. Blue line represents the control experiment where only GSK1016790A (5nM) was added to the basal bathing media (time, t= 0). The symbols denote the means of 6 experiments ± SE. 2mV pulses were induced every 200 seconds and the current displacement during the pulse was used to calculate the transepithelial resistance via Ohm's law. (C) TER plots: After stabilization, acetazolamide (100µM) was added either to the apical or basal bathing media (time, t= 0) and GSK1016790A (5nM) was added to the basal bathing media (time, t= 600). The symbols denote the means of 6 experiments ± SE. Blue line represents the control experiment where only GSK1016790A (5nM) was added to the basal bathing media (time, t= 600). The symbols denote the means of 6 experiments ± SE. (D) TER plots: After stabilization, GSK1016790A (5nM) was added to the basal bathing media (time, t= 0) and acetazolamide (100µM) was added either to the apical or basal bathing media (time, t= 600). The symbols denote the means of 6 experiments ± SE. Blue line represents the control experiment where only GSK1016790A (5nM) was added to the basal bathing media (time, t= 0). The symbols denote the means of 6 experiments ± SE.

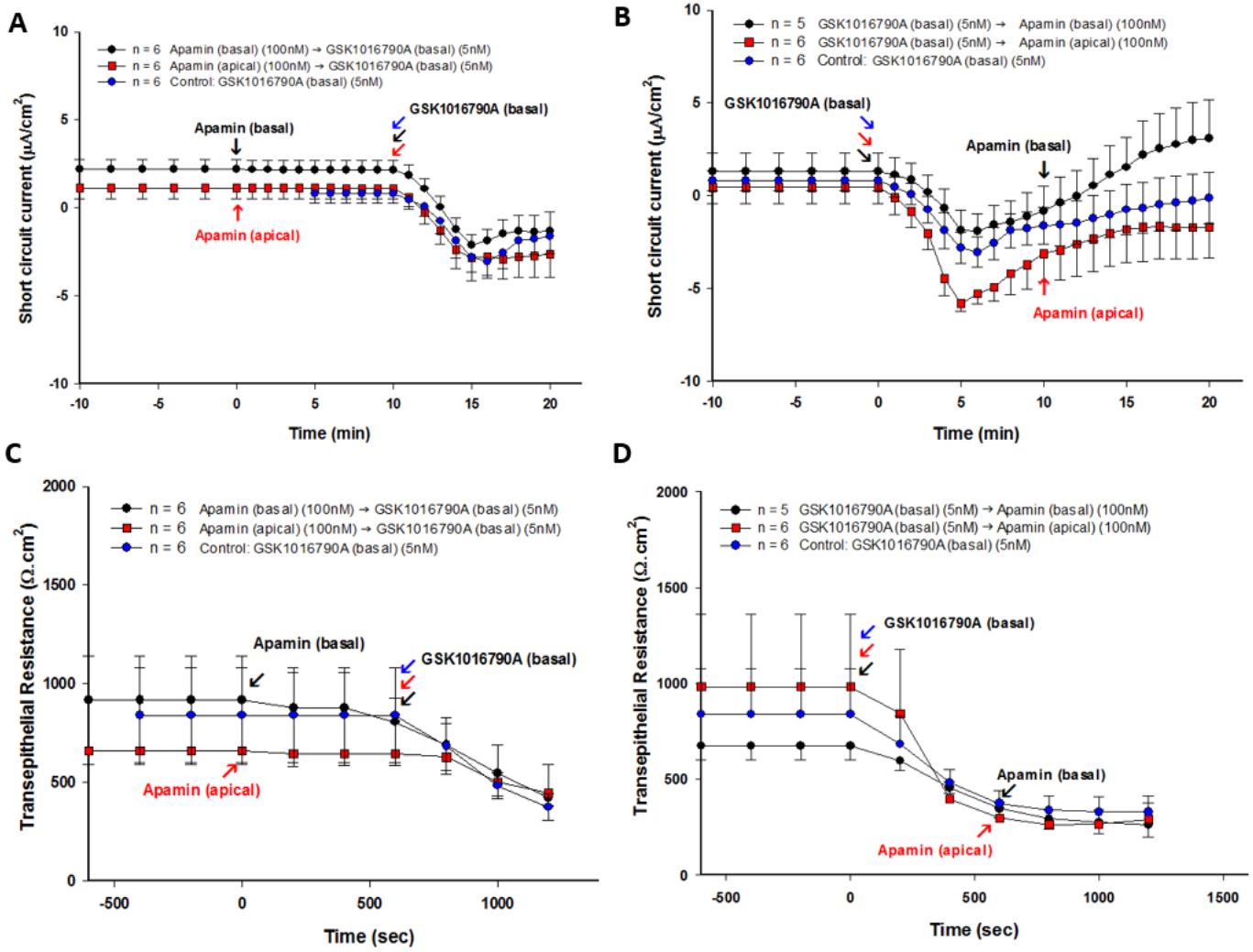
A
n = 6 Apamin (basal) (100nM) → GSK1016790A (basal) (5nM)
n = 6 Apamin (apical) (100nM) → GSK1016790A (basal) (5nM)
n = 6 Control: GSK1016790A (basal) (5nM)
Apamin (basal)
GSK1016790A (basal)
Apamin (apical)
Short circuit current (μA/cm²)
Time (min)
B
n = 5 GSK1016790A (basal) (5nM) → Apamin (basal) (100nM)
n = 6 GSK1016790A (basal) (5nM) → Apamin (apical) (100nM)
n = 6 Control: GSK1016790A (basal) (5nM)
GSK1016790A (basal)
Apamin (basal)
Apamin (apical)
Short circuit current (μA/cm²)
Time (min)
C
n = 6 Apamin (basal) (100nM) → GSK1016790A (basal) (5nM)
n = 6 Apamin (apical) (100nM) → GSK1016790A (basal) (5nM)
n = 6 Control: GSK1016790A (basal) (5nM)
Apamin (basal)
GSK1016790A (basal)
Apamin (apical)
Transepithelial Resistance (Ω.cm²)
Time (sec)
D
n = 5 GSK1016790A (basal) (5nM) → Apamin (basal) (100nM)
n = 6 GSK1016790A (basal) (5nM) → Apamin (apical) (100nM)
n = 6 Control: GSK1016790A (basal) (5nM)
GSK1016790A (basal)
Apamin (basal)
Apamin (apical)
Transepithelial Resistance (Ω.cm²)
Time (sec)

Figure 3.9

Figure 3.9: TRPV4 mediated ion flux and TER decline is not effected by apamin. PCP-R cells were grown on permeable Transwell membranes for 10 to 12 days to reach confluence, excised, mounted in an Ussing chamber, and allowed to develop a stable basal short-circuit current (SCC). SCC is a measure of net transepithelial ion transport. (A) SCC plots: After stabilization, apamin (100nM) was added either to the apical or basal bathing media (time, t= 0) and GSK1016790A (5nM) was added to the basal bathing media (time, t= 10). The symbols denote the means of 6 experiments ± SE. Blue line represents the control experiment where only GSK1016790A (5nM) was added to the basal bathing media (time, t= 10). The symbols denote the means of 6 experiments ± SE. (B) SCC plots: After stabilization, GSK1016790A (5nM) was added to the basal bathing media (time, t= 0) and apamin (100nM) was added either to the apical or basal bathing media (time, t= 10). The symbols denote the means of 5 or 6 experiments ± SE. Blue line represents the control experiment where only GSK1016790A (5nM) was added to the basal bathing media (time, t= 0). The symbols denote the means of 6 experiments ± SE. 2mV pulses were induced every 200 seconds and the current displacement during the pulse was used to calculate the transepithelial resistance via Ohm's law. (C) TER plots: After stabilization, apamin (100nM) was added either to the apical or basal bathing media (time, t= 0) and GSK1016790A (5nM) was added to the basal bathing media (time, t= 600). The symbols denote the means of 6 experiments ± SE. Blue line represents the control experiment where only GSK1016790A (5nM) was added to the basal bathing media (time, t= 600). The symbols denote the means of 6 experiments ± SE. (D) TER plots: After stabilization, GSK1016790A (5nM) was added to the basal bathing media (time, t= 0) and apamin (100nM) was added either to the apical or basal bathing media (time, t= 600). The symbols denote the means of 5 or 6 experiments ± SE. Blue line represents the control experiment where only GSK1016790A (5nM) was added to the basal bathing media (time, t= 0). The symbols denote the means of 6 experiments ± SE.

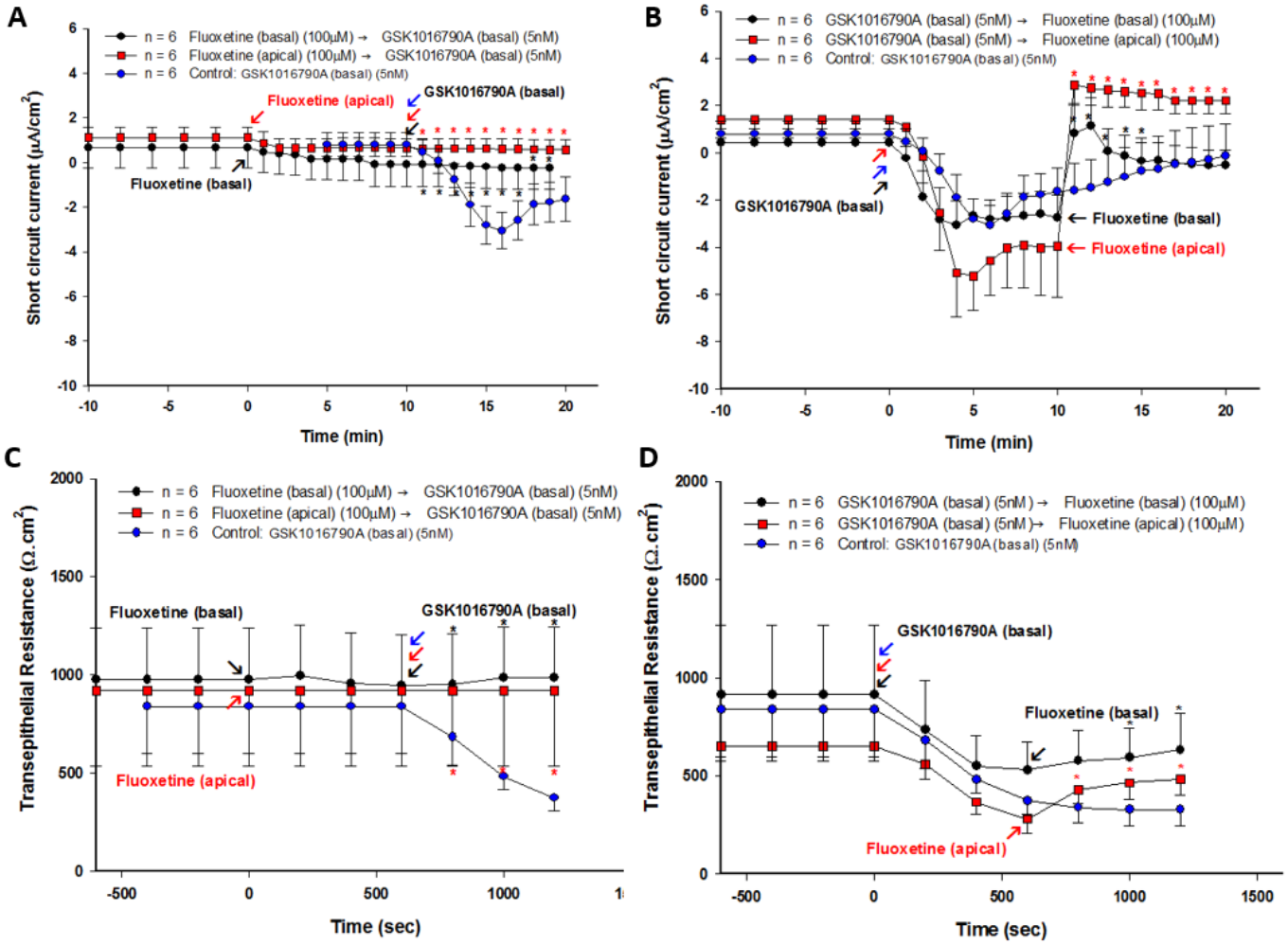
A
n = 6 Fluoxetine (basal) (100µM) → GSK1016790A (basal) (5nM)
n = 6 Fluoxetine (apical) (100µM) → GSK1016790A (basal) (5nM)
n = 6 Control: GSK1016790A (basal) (5nM)
Fluoxetine (apical)
GSK1016790A (basal)
Fluoxetine (basal)
Short circuit current (µA/cm²)
Time (min)
B
n = 6 GSK1016790A (basal) (5nM) → Fluoxetine (basal) (100µM)
n = 6 GSK1016790A (basal) (5nM) → Fluoxetine (apical) (100µM)
n = 6 Control: GSK1016790A (basal) (5nM)
GSK1016790A (basal)
Fluoxetine (basal)
Fluoxetine (apical)
Short circuit current (µA/cm²)
Time (min)
C
n = 6 Fluoxetine (basal) (100µM) → GSK1016790A (basal) (5nM)
n = 6 Fluoxetine (apical) (100µM) → GSK1016790A (basal) (5nM)
n = 6 Control: GSK1016790A (basal) (5nM)
Fluoxetine (basal)
GSK1016790A (basal)
Fluoxetine (apical)
Transepithelial Resistance (Ω.cm²)
Time (sec)
D
n = 6 GSK1016790A (basal) (5nM) → Fluoxetine (basal) (100µM)
n = 6 GSK1016790A (basal) (5nM) → Fluoxetine (apical) (100µM)
n = 6 Control: GSK1016790A (basal) (5nM)
GSK1016790A (basal)
Fluoxetine (basal)
Fluoxetine (apical)
Transepithelial Resistance (Ω.cm²)
Time (sec)

Figure 3.10

Figure 3.10: TRPV4 mediated ion flux is fully reversed and TER decline is partially reversed by fluoxetine. PCP-R cells were grown on permeable Transwell membranes for 10 to 12 days to reach confluence, excised, mounted in an Ussing chamber, and allowed to develop a stable basal short-circuit current (SCC). SCC is a measure of net transepithelial ion transport. (A) SCC plots: After stabilization, fluoxetine (100µM) was added either to the apical or basal bathing media (time, t= 0) and GSK1016790A (5nM) was added to the basal bathing media (time, t= 10). The symbols denote the means of 6 experiments ± SE. Blue line represents the control experiment where only GSK1016790A (5nM) was added to the basal bathing media (time, t= 10). The symbols denote the means of 6 experiments ± SE. (*) denotes statistically significant SCC change compared to the control experiments ($p \leq 0.05$; Student's t-test). (B) SCC plots: After stabilization, GSK1016790A (5nM) was added to the basal bathing media (time, t= 0) and fluoxetine (100µM) was added either to the apical or basal bathing media (time, t= 10). The symbols denote the means of 6 experiments ± SE. Blue line represents the control experiment where only GSK1016790A (5nM) was added to the basal bathing media (time, t= 0). The symbols denote the means of 6 experiments ± SE. (*) denotes statistically significant SCC change compared to the control experiments ($p \leq 0.05$; Student's t-test). 2mV pulses were induced every 200 seconds and the current displacement during the pulse was used to calculate the transepithelial resistance via Ohm's law. (C) TER plots: After stabilization, fluoxetine (100µM) was added either to the apical or basal bathing media (time, t= 0) and GSK1016790A (5nM) was added to the basal bathing media (time, t= 600). The symbols denote the means of 6 experiments ± SE. Blue line represents the control experiment where only GSK1016790A (5nM) was added to the basal bathing media (time, t= 600). The symbols denote the means of 6 experiments ± SE. (*) denotes statistically significant TER change compared to the control experiments ($p \leq 0.05$; Student's t-test). (D) TER plots: After stabilization, GSK1016790A (5nM) was added to the basal bathing media (time, t= 0) and fluoxetine (100µM) was added either to the apical or basal bathing media (time, t= 600). The symbols denote the means of 6 experiments ± SE. Blue line represents the control experiment where only GSK1016790A (5nM) was added to the basal bathing media (time, t= 0). The symbols denote the means of 6 experiments ± SE. (*) denotes statistically significant TER change compared to the control experiments ($p \leq 0.05$; Student's t-test).

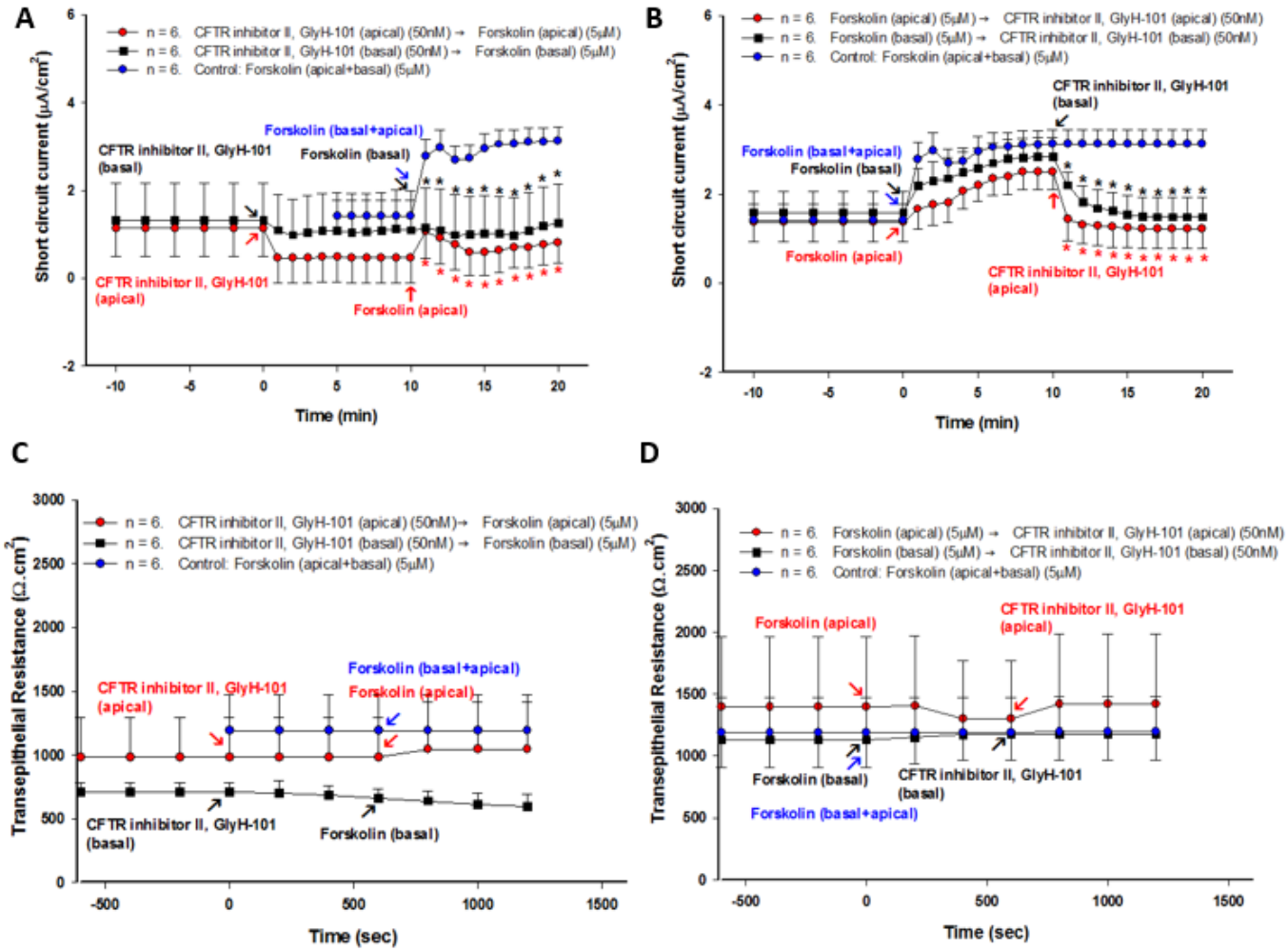
A
n = 6. CFTR inhibitor II, GlyH-101 (apical) (50nM) → Forskolin (apical) (5μM)
n = 6. CFTR inhibitor II, GlyH-101 (basal) (50nM) → Forskolin (basal) (5μM)
n = 6. Control: Forskolin (apical+basal) (5μM)
Short circuit current (μA/cm²)
Forskolin (basal+apical)
CFTR inhibitor II, GlyH-101 (basal)
Forskolin (basal)
CFTR inhibitor II, GlyH-101 (apical)
Forskolin (apical)
Time (min)
B
n = 6. Forskolin (apical) (5μM) → CFTR inhibitor II, GlyH-101 (apical) (50nM)
n = 6. Forskolin (basal) (5μM) → CFTR inhibitor II, GlyH-101 (basal) (50nM)
n = 6. Control: Forskolin (apical+basal) (5μM)
Short circuit current (μA/cm²)
CFTR inhibitor II, GlyH-101 (basal)
Forskolin (basal+apical)
Forskolin (basal)
Forskolin (apical)
CFTR inhibitor II, GlyH-101 (apical)
Time (min)
C
n = 6. CFTR inhibitor II, GlyH-101 (apical) (50nM)→ Forskolin (apical) (5μM)
n = 6. CFTR inhibitor II, GlyH-101 (basal) (50nM) → Forskolin (basal) (5μM)
n = 6. Control: Forskolin (apical+basal) (5μM)
Transepithelial Resistance (Ω.cm²)
CFTR inhibitor II, GlyH-101 (apical)
Forskolin (basal+apical)
Forskolin (apical)
CFTR inhibitor II, GlyH-101 (basal)
Forskolin (basal)
Time (sec)
D
n = 6. Forskolin (apical) (5μM) → CFTR inhibitor II, GlyH-101 (apical) (50nM)
n = 6. Forskolin (basal) (5μM) → CFTR inhibitor II, GlyH-101 (basal) (50nM)
n = 6. Control: Forskolin (apical+basal) (5μM)
Transepithelial Resistance (Ω.cm²)
Forskolin (apical)
CFTR inhibitor II, GlyH-101 (apical)
Forskolin (basal)
CFTR inhibitor II, GlyH-101 (basal)
Forskolin (basal+apical)
Time (sec)

Figure 3.11

Figure 3.11: CFTR is activated by forskolin induced cAMP. PCP-R cells were grown on permeable Transwell membranes for 10 to 12 days to reach confluence, excised, mounted in an Ussing chamber, and allowed to develop a stable basal short-circuit current (SCC). SCC is a measure of net transepithelial ion transport. (A) SCC plots: After stabilization, CFTR inhibitor II, GlyH-101 (50nM) was added either to the apical or basal bathing media (time, t= 0) and forskolin (5µM) was added either to the apical or basal bathing media (time, t= 10). The symbols denote the means of 6 experiments ± SE. Blue line represents the control experiment where only forskolin (5µM) was added either to the apical or basal bathing media (time, t= 10). The symbols denote the means of 6 experiments ± SE. (*) denotes statistically significant SCC change compared to the control experiments ($p \leq 0.05$; Student's t-test). (B) SCC plots: After stabilization, forskolin (5µM) was added either to the apical or basal bathing media (time, t= 0) and CFTR inhibitor II, GlyH-101 (50nM) was added either to the apical or basal bathing media (time, t= 10). The symbols denote the means of 6 experiments ± SE. Blue line represents the control experiment where only forskolin (5µM) was added either to the apical or basal bathing media (time, t= 0). The symbols denote the means of 6 experiments ± SE. (*) denotes statistically significant SCC change compared to the control experiments ($p \leq 0.05$; Student's t-test). 2mV pulses were induced every 200 seconds and the current displacement during the pulse was used to calculate the transepithelial resistance via Ohm's law. (C) TER plots: After stabilization, CFTR inhibitor II, GlyH-101 (50nM) was added either to the apical or basal bathing media (time, t= 0) and forskolin (5µM) was added either to the apical or basal bathing media (time, t= 600). The symbols denote the means of 6 experiments ± SE. Blue line represents the control experiment where only forskolin (5µM) was added either to the apical or basal bathing media (time, t= 600). The symbols denote the means of 6 experiments ± SE. (D) TER plots: After stabilization, forskolin (5µM) was added either to the apical or basal bathing media (time, t= 0) and CFTR inhibitor II, GlyH-101 (50nM) was added to the basal bathing media (time, t= 600). The symbols denote the means of 6 experiments ± SE. Blue line represents the control experiment where only forskolin (5µM) was added either to the apical or basal bathing media (time, t= 0). The symbols denote the means of 6 experiments ± SE.

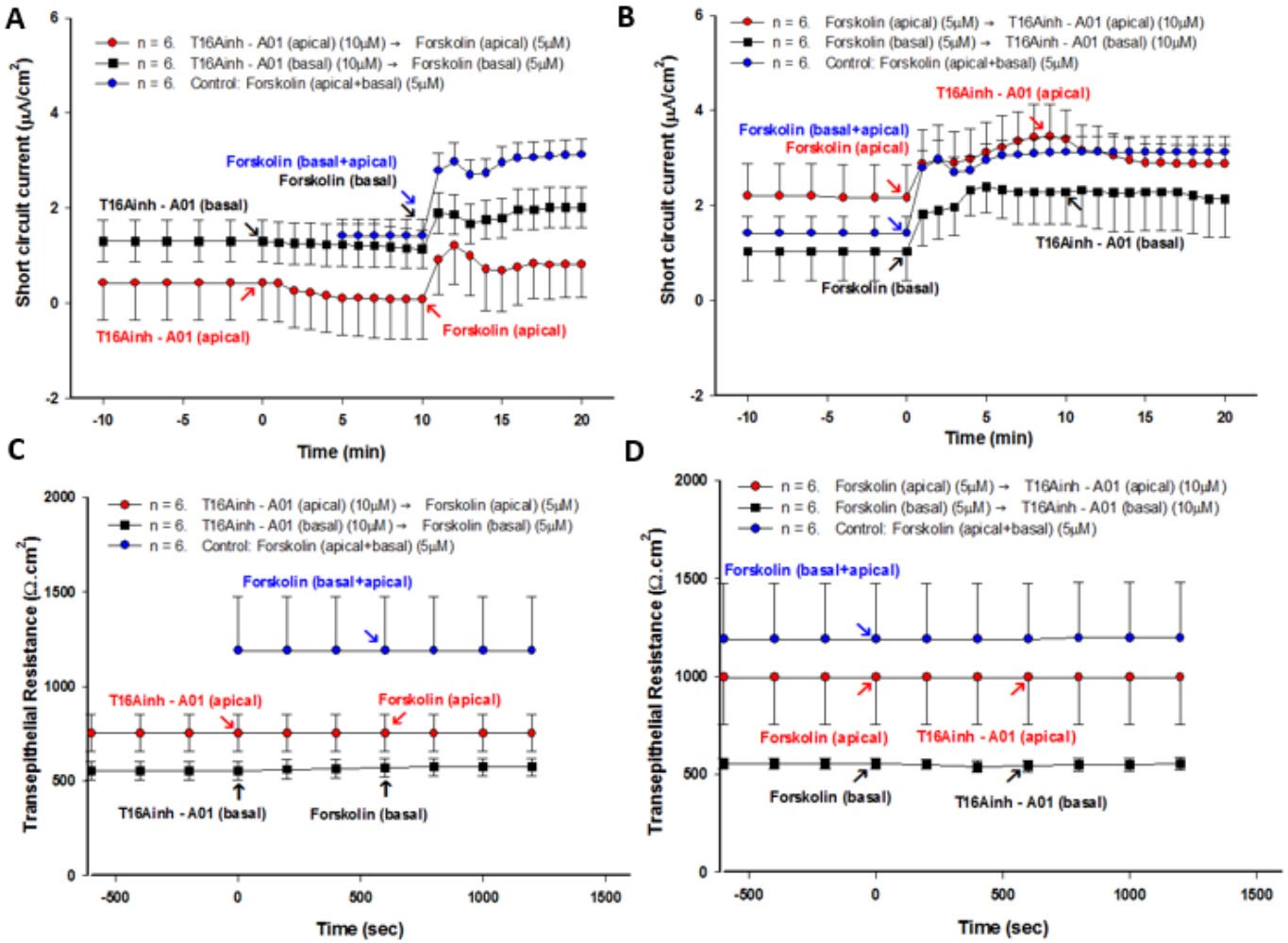
A
n = 6. T16Ainh - A01 (apical) (10μM) → Forskolin (apical) (5μM)
n = 6. T16Ainh - A01 (basal) (10μM) → Forskolin (basal) (5μM)
n = 6. Control: Forskolin (apical+basal) (5μM)
Short circuit current (μA/cm²)
Forskolin (basal+apical)
Forskolin (basal)
T16Ainh - A01 (basal)
T16Ainh - A01 (apical)
Forskolin (apical)
Time (min)
B
n = 6. Forskolin (apical) (5μM) → T16Ainh - A01 (apical) (10μM)
n = 6. Forskolin (basal) (5μM) → T16Ainh - A01 (basal) (10μM)
n = 6. Control: Forskolin (apical+basal) (5μM)
Short circuit current (μA/cm²)
T16Ainh - A01 (apical)
Forskolin (basal+apical)
Forskolin (apical)
T16Ainh - A01 (basal)
Forskolin (basal)
Time (min)
C
n = 6. T16Ainh - A01 (apical) (10μM) → Forskolin (apical) (5μM)
n = 6. T16Ainh - A01 (basal) (10μM) → Forskolin (basal) (5μM)
n = 6. Control: Forskolin (apical+basal) (5μM)
Transepithelial Resistance (Ω.cm²)
Forskolin (basal+apical)
T16Ainh - A01 (apical)
Forskolin (apical)
T16Ainh - A01 (basal)
Forskolin (basal)
Time (sec)
D
n = 6. Forskolin (apical) (5μM) → T16Ainh - A01 (apical) (10μM)
n = 6. Forskolin (basal) (5μM) → T16Ainh - A01 (basal) (10μM)
n = 6. Control: Forskolin (apical+basal) (5μM)
Transepithelial Resistance (Ω.cm²)
Forskolin (basal+apical)
Forskolin (apical)
T16Ainh - A01 (apical)
Forskolin (basal)
T16Ainh - A01 (basal)
Time (sec)

Figure 3.12

Figure 3.12: TMEM16A is not activated by forskolin and does not affect the TER. PCP-R cells were grown on permeable Transwell membranes for 10 to 12 days to reach confluence, excised, mounted in an Ussing chamber, and allowed to develop a stable basal short-circuit current (SCC). SCC is a measure of net transepithelial ion transport. (A) SCC plots: After stabilization, T16Ainh – A01 (10µM) was added either to the apical or basal bathing media (time, t= 0) and forskolin (5µM) was added either to the apical or basal bathing media (time, t= 10). The symbols denote the means of 6 experiments ± SE. Blue line represents the control experiment where only forskolin (5µM) was added either to the apical or basal bathing media (time, t= 10). The symbols denote the means of 6 experiments ± SE. (B) SCC plots: After stabilization, forskolin (5µM) was added either to the apical or basal bathing media (time, t= 0) and T16Ainh – A01 (10µM) was added either to the apical or basal bathing media (time, t= 10). The symbols denote the means of 6 experiments ± SE. Blue line represents the control experiment where only forskolin (5µM) was added either to the apical or basal bathing media (time, t= 0). The symbols denote the means of 6 experiments ± SE. 2mV pulses were induced every 200 seconds and the current displacement during the pulse was used to calculate the transepithelial resistance via Ohm's law. (C) TER plots: After stabilization, T16Ainh – A01 (10µM) was added either to the apical or basal bathing media (time, t= 0) and forskolin (5µM) was added either to the apical or basal bathing media (time, t= 600). The symbols denote the means of 6 experiments ± SE. Blue line represents the control experiment where only forskolin (5µM) was added either to the apical or basal bathing media (time, t= 600). The symbols denote the means of 6 experiments ± SE. (D) TER plots: After stabilization, forskolin (5µM) was added either to the apical or basal bathing media (time, t= 0) and T16Ainh – A01 (10µM) was added either to the apical or basal bathing media (time, t= 600). The symbols denote the means of 6 experiments ± SE. Blue line represents the control experiment where only forskolin (5µM) was added either to the apical or basal bathing media (time, t= 0). The symbols denote the means of 6 experiments ± SE.

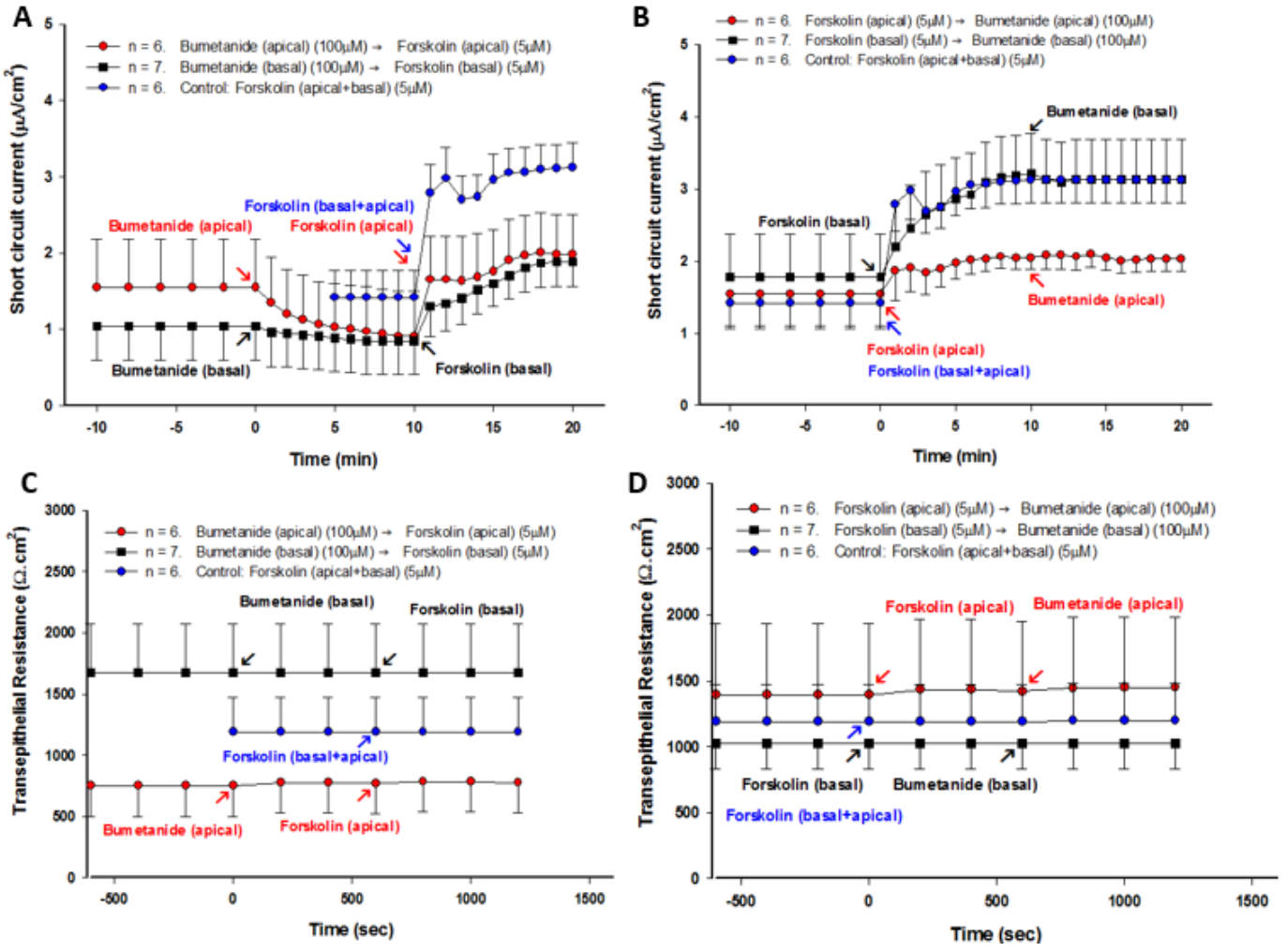
A
n = 6. Bumetanide (apical) (100μM) → Forskolin (apical) (5μM)
n = 7. Bumetanide (basal) (100μM) → Forskolin (basal) (5μM)
n = 6. Control: Forskolin (apical+basal) (5μM)
Short circuit current (μA/cm²)
Bumetanide (apical)
Forskolin (basal+apical)
Forskolin (apical)
Bumetanide (basal)
Forskolin (basal)
Time (min)
B
n = 6. Forskolin (apical) (5μM) → Bumetanide (apical) (100μM)
n = 7. Forskolin (basal) (5μM) → Bumetanide (basal) (100μM)
n = 6. Control: Forskolin (apical+basal) (5μM)
Short circuit current (μA/cm²)
Bumetanide (basal)
Forskolin (basal)
Bumetanide (apical)
Forskolin (apical)
Forskolin (basal+apical)
Time (min)
C
n = 6. Bumetanide (apical) (100μM) → Forskolin (apical) (5μM)
n = 7. Bumetanide (basal) (100μM) → Forskolin (basal) (5μM)
n = 6. Control: Forskolin (apical+basal) (5μM)
Transepithelial Resistance (Ω.cm²)
Bumetanide (basal)
Forskolin (basal)
Forskolin (basal+apical)
Bumetanide (apical)
Forskolin (apical)
Time (sec)
D
n = 6. Forskolin (apical) (5μM) → Bumetanide (apical) (100μM)
n = 7. Forskolin (basal) (5μM) → Bumetanide (basal) (100μM)
n = 6. Control: Forskolin (apical+basal) (5μM)
Transepithelial Resistance (Ω.cm²)
Forskolin (apical)
Bumetanide (apical)
Forskolin (basal)
Bumetanide (basal)
Forskolin (basal+apical)
Time (sec)

Figure 3.13

Figure 3.13: NKCC1 is apical in PCP-R. PCP-R cells were grown on permeable Transwell membranes for 10 to 12 days to reach confluence, excised, mounted in an Ussing chamber, and allowed to develop a stable basal short-circuit current (SCC). SCC is a measure of net transepithelial ion transport. (A) SCC plots: After stabilization, bumetanide (100µM) was added either to the apical or basal bathing media (time, t= 0) and forskolin (5µM) was added either to the apical or basal bathing media (time, t= 10). The symbols denote the means of 6 or 7 experiments ± SE. Blue line represents the control experiment where only forskolin (5µM) was added either to the apical or basal bathing media (time, t= 10). The symbols denote the means of 6 experiments ± SE. (B) SCC plots: After stabilization, forskolin (5µM) was added either to the apical or basal bathing media (time, t= 0) and bumetanide (100µM) was added either to the apical or basal bathing media (time, t= 10). The symbols denote the means of 6 or 7 experiments ± SE. Blue line represents the control experiment where only forskolin (5µM) was added either to the apical or basal bathing media (time, t= 0). The symbols denote the means of 6 experiments ± SE. 2mV pulses were induced every 200 seconds and the current displacement during the pulse was used to calculate the transepithelial resistance via Ohm's law. (C) TER plots: After stabilization, bumetanide (100µM) was added either to the apical or basal bathing media (time, t= 0) and forskolin (5µM) was added either to the apical or basal bathing media (time, t= 600). The symbols denote the means of 6 or 7 experiments ± SE. Blue line represents the control experiment where only forskolin (5µM) was added either to the apical or basal bathing media (time, t= 600). The symbols denote the means of 6 experiments ± SE. (D) TER plots: After stabilization, forskolin (5µM) was added either to the apical or basal bathing media (time, t= 0) and bumetanide (100µM) was added either to the apical or basal bathing media (time, t= 600). The symbols denote the means of 6 or 7 experiments ± SE. Blue line represents the control experiment where only forskolin (5µM) was added either to the apical or basal bathing media (time, t= 0). The symbols denote the means of 6 experiments ± SE.

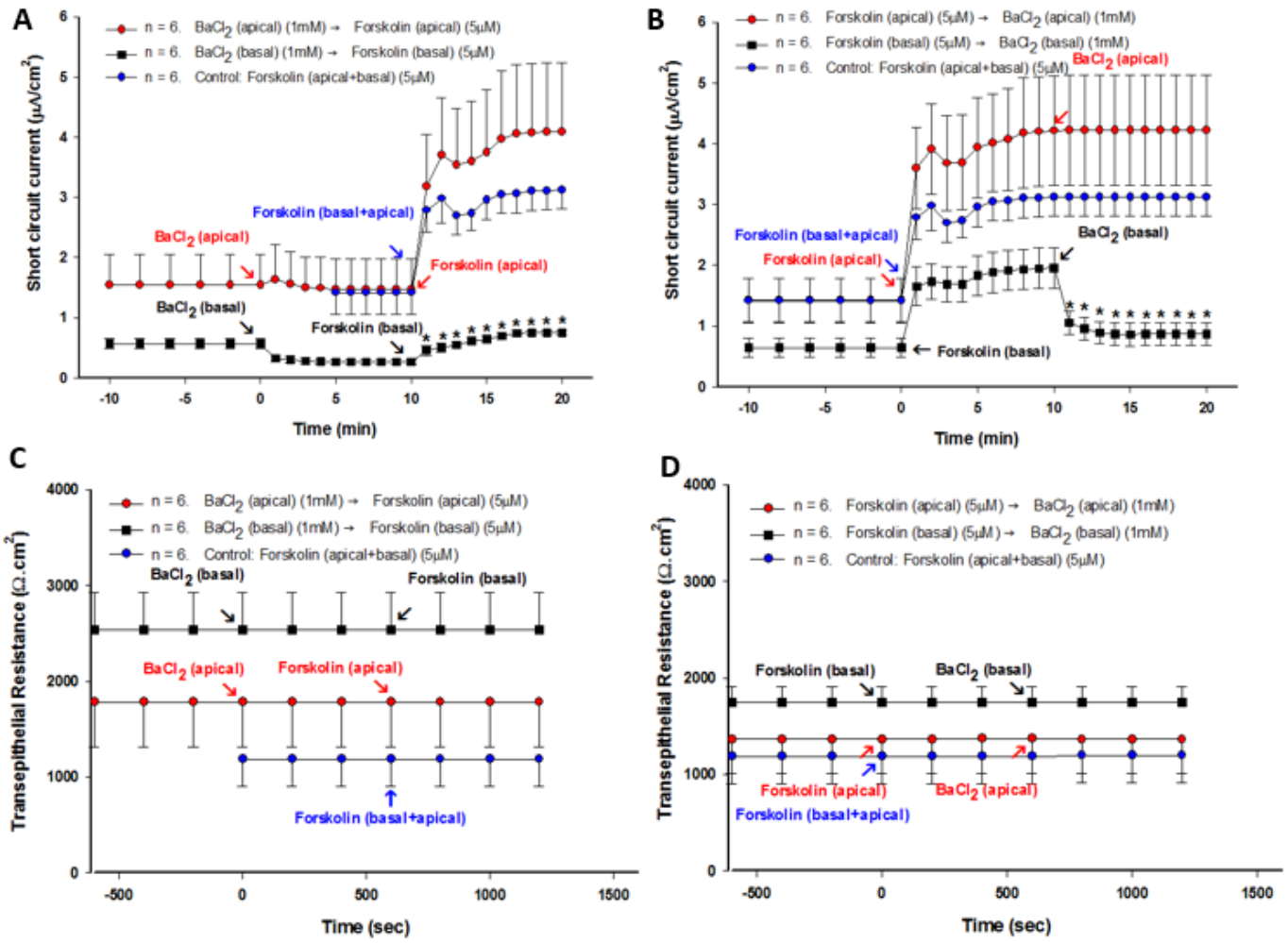
A
n = 6. BaCl2 (apical) (1mM) → Forskolin (apical) (5μM)
n = 6. BaCl2 (basal) (1mM) → Forskolin (basal) (5μM)
n = 6. Control: Forskolin (apical+basal) (5μM)
Short circuit current (μA/cm2)
BaCl2 (apical)
Forskolin (basal+apical)
Forskolin (apical)
BaCl2 (basal)
Forskolin (basal)
Time (min)
B
n = 6. Forskolin (apical) (5μM) → BaCl2 (apical) (1mM)
n = 6. Forskolin (basal) (5μM) → BaCl2 (basal) (1mM)
n = 6. Control: Forskolin (apical+basal) (5μM)
Short circuit current (μA/cm2)
BaCl2 (apical)
Forskolin (basal+apical)
Forskolin (apical)
BaCl2 (basal)
Forskolin (basal)
Time (min)
C
n = 6. BaCl2 (apical) (1mM) → Forskolin (apical) (5μM)
n = 6. BaCl2 (basal) (1mM) → Forskolin (basal) (5μM)
n = 6. Control: Forskolin (apical+basal) (5μM)
Transepithelial Resistance (Ω.cm2)
BaCl2 (basal)
Forskolin (basal)
BaCl2 (apical)
Forskolin (apical)
Forskolin (basal+apical)
Time (sec)
D
n = 6. Forskolin (apical) (5μM) → BaCl2 (apical) (1mM)
n = 6. Forskolin (basal) (5μM) → BaCl2 (basal) (1mM)
n = 6. Control: Forskolin (apical+basal) (5μM)
Transepithelial Resistance (Ω.cm2)
Forskolin (basal)
BaCl2 (basal)
Forskolin (apical)
BaCl2 (apical)
Forskolin (basal+apical)
Time (sec)

Figure 3.14

Figure 3.14: Forskolin mediated ion flux is reversed by $BaCl_2$ when added on the basolateral side of the membrane. TER is not effected. PCP-R cells were grown on permeable Transwell membranes for 10 to 12 days to reach confluence, excised, mounted in an Ussing chamber, and allowed to develop a stable basal short-circuit current (SCC). SCC is a measure of net transepithelial ion transport. (A) SCC plots: After stabilization, $BaCl_2$ (1mM) was added either to the apical or basal bathing media (time, t= 0) and forskolin (5µM) was added either to the apical or basal bathing media (time, t= 10). The symbols denote the means of 6 experiments ± SE. Blue line represents the control experiment where only forskolin (5µM) was added either to the apical or basal bathing media (time, t= 10). The symbols denote the means of 6 experiments ± SE. (*) denotes statistically significant SCC change compared to the control experiments ($p \leq 0.05$; Student's t-test). (B) SCC plots: After stabilization, forskolin (5µM) was added either to the apical or basal bathing media (time, t= 0) and $BaCl_2$ (1mM) was added either to the apical or basal bathing media (time, t= 10). The symbols denote the means of 6 experiments ± SE. Blue line represents the control experiment where only forskolin (5µM) was added either to the apical or basal bathing media (time, t= 0). The symbols denote the means of 6 experiments ± SE. (*) denotes statistically significant SCC change compared to the control experiments ($p \leq 0.05$; Student's t-test). 2mV pulses were induced every 200 seconds and the current displacement during the pulse was used to calculate the transepithelial resistance via Ohm's law. (C) TER plots: After stabilization, $BaCl_2$ (1mM) was added either to the apical or basal bathing media (time, t= 0) and forskolin (5µM) was added either to the apical or basal bathing media (time, t= 600). The symbols denote the means of 6 experiments ± SE. Blue line represents the control experiment where only forskolin (5µM) was added either to the apical or basal bathing media (time, t= 600). The symbols denote the means of 6 experiments ± SE. (D) TER plots: After stabilization, forskolin (5µM) was added either to the apical or basal bathing media (time, t= 0) and $BaCl_2$ (1mM) was added either to the apical or basal bathing media (time, t= 600). The symbols denote the means of 6 experiments ± SE. Blue line represents the control experiment where only forskolin (5µM) was added either to the apical or basal bathing media (time, t= 0). The symbols denote the means of 6 experiments ± SE.

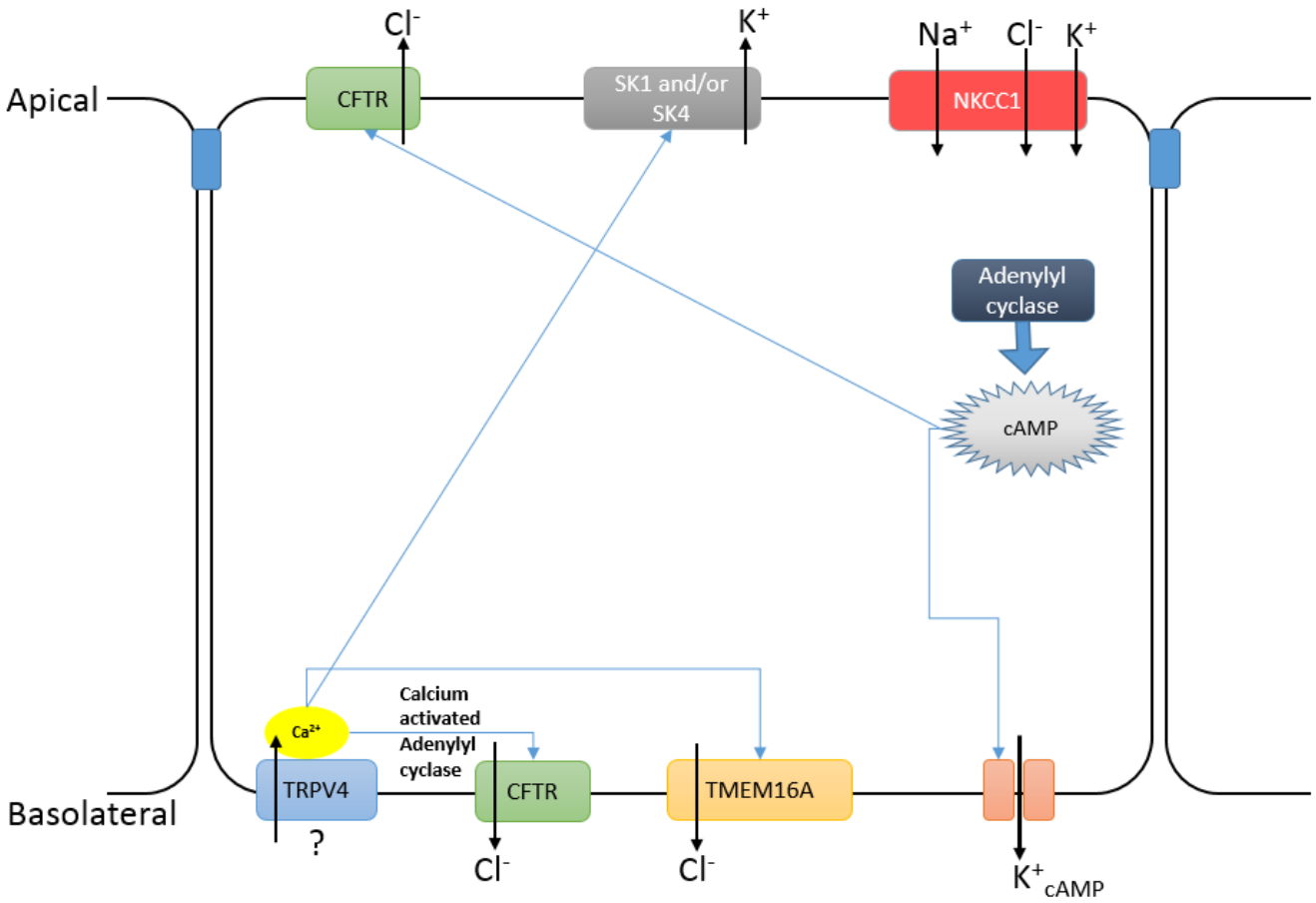

Figure 4.1: Schematic representation of the ion transporters in choroid plexus. TRPV4 might be on the basal membrane. CFTR might be located in both side of the membrane, whereas TMEM16A is basal and SK1 and/or SK4 might be located in the apical membrane. NKCC1 might also be located in the apical membrane. cAMP activated potassium channels are located in the basolateral membrane.